UNIVERSITY OF
KWAZULU-NATAL

INYUVESI
YAKWAZULU-NATALI

The cytotoxic effects of fumonisin B_1 in human kidney cells and the ability of allicin to ameliorate these effects

By

Nomalungelo Nothando Felicity Mahlalela (218063202)

BSc. (Medical sciences, University of Limpopo)

Submitted in fulfilment of the requirements for the degree of MMedSci. in the

Discipline of Medical Biochemistry and Chemical Pathology

School of Laboratory Medicine and Medical Sciences

College of Health Sciences

University of KwaZulu-Natal, Durban

2019

DECLARATION

I Miss NNF Mahlalela declare that:

1. This dissertation contains original work done by the author and has not been submitted to UKZN or any other tertiary institution for the purposes of obtaining an academic qualification, whether by myself or any other party. The use of work by others has been duly acknowledged in the text.

2. The research described in this study was carried out in the Department of Medical Biochemistry and Chemical Pathology, School of Laboratory Medicine and Medical Science, Faculty of Health Sciences, University of KwaZulu-Natal, Durban, under the supervision of Dr R.B Khan.

Signed:  Date: 19 July 2019

ACKNOWLEDGEMENTS

Dr Rene B. Khan

To the one person whose wisdom and guidance knows no bounds. You have groomed me not only into a better scientist but a better person. You have inspired me to be the best version of myself with every waking day. Thank you for the time you invested in me.

My brother

You have been the embodiment of my strength from the beginning of it all. Thank you for always being in my corner, for being my home. You have supported me through it all, I love you big bro.

Abba Armooh

Thank you for so many things but mostly for being my peace, when school got hectic and stress took over; you always knew just what to say. Your bottomless support carried me through.

Thobeka Madide

Thank you for your constant encouragement and support. I am grateful for your friendship.

Department of Medical Biochemistry

To the entire staff of the department of Medical biochemistry, thank you for your patience, unwavering support and assistance during the course of this project.

University of KwaZulu-Natal College of Health Sciences and National Research Foundation

I appreciate the awarded scholarships that financially facilitated the completion of this degree.

ABBREVIATIONS

AGE	Aged garlic extract
Apaf1	Apoptotic-protease-activating-factor-1
iROS	Intercellular reactive oxygen species
ATP	Adenosine triphosphate
Bax	Bcl-2-associated X
BCA	Bicinchoninic acid
Bcl-2	B-cell lymphoma/leukemia-2
BH3	Bcl-2 homology domain 3
BHT	Butylated hydroxytoluene
BSA	Bovine serum albumin
CCM	Complete culture medium
cDNA	Complimentary DNA
CO_2	Carbon dioxide
$CuSO_4$	Copper sulphate
DADS	Diallyl disulfide
DAS	Diallyl sulfide
DAT	Diallyl trisulfide
DD	Death domain
dH_2O	De-ionised water
DISC	Death inducing signalling complex
DMEM	Dulbecco's Modified Eagle's Medium

DMSO	Dimethyl sulphoxide
DNA	Deoxymethylribose nucleic acid
DNase	Deoxyribonuclease
DNMT	DNA methyltransferase
EDTA	Ethylenediaminetetraacetic acid
Ex	Excitation wavelength
Em	Emission wavelength
FB_1	Fumonisin B_1
GPx	Gluathione peroxidase
GSH	Glutathione
H_2O	Water
H_2O_2	Hydrogen peroxide
H_3PO_4	Phosphoric acid
HCl	Hydrochloric acid
HEK293	Human embryonic kidney cells
IARC	International agency for research on cancer
IC_{50}	Median Inhibition Concentration
iCAD	Inhibitors of caspase DNase
LDH	Lactate dehydrogenase
LEM	Leukoencephalomalacia
LLC-PK_1	Pig kidney epithelial cells
LMPA	Low melting point agarose
MDA	Malondialdehyde

miRNA	MicroRNA
MTT	Methyl tetrazolium
NaCl	Sodium chloride
NaOH	Sodium hydroxide
NEDD	N-(1-naphthyl)ethylenediamine
Nm	Nanometer
Nrf2	Nuclear factor erythroid 2 (NFE2)-related factor 2
NTD	Neural tube defect
O_2^-	Superoxide ion
OC	Oesophageal cancer
PBS	Phosphate-buffered saline
PCR	Polymerase chain reaction
PFA	Paraformaldehyde
Prxs	Peroxidase
qPCR	Quantitative polymerase chain reaction
RLU	Relative light unit
RNA	Ribonucleic acid
RNA	Ribose nucleic acid
RNS	Reactive nitrogen species
ROS	Reactive oxygen species
RT	Room temperature
SAC	S-allylcysteine
SAM	S-adenosyl methionine

SCGE	Single cell gel electrophoresis
SDH	succinate dehydrogenase
SDS-PAGE	Sodium dodecyl sulphate - polyacrylamide gel electrophoresis
SOD	Superoxide dismutase
SULF	Sulfanilamide
TBA	Thiobarbituric Acid
TBARS	Thiobarbituric Acid Reactive Substances
tBID	Truncated BH3 interacting-domain death agonist
TCA	Tricarboxylic acid
TNF	Tumor necrosis factor
TTBS	Tris-buffered saline containing 0.5% Tween20
VCl_3	Vanadium (III) chloride

TABLE OF CONTENTS

LIST OF FIGURES

ABSTRACT

Fumonisin B_1 (FB_1) is a widespread contaminant of crops and is produced as a secondary metabolite of fungi. It has been found to disrupt sphingolipid metabolism, cause epigenetic modifications and induce cellular toxicity that can manifest through oxidative stress and apoptosis. Although implicated in animal toxicity including kidney cancer in rats, FB_1 effects in the human kidney have not been explored. Allicin is a biological component of garlic that has been widely studied for its health benefits including its anti-cancer and antioxidant properties. This study evaluated allicin as a possible therapeutic measure for FB_1-induced cytotoxicity in Hek293 cells. Both FB_1 and allicin decreased cellular viability (MTT assay) in a dose-dependent manner and generated IC_{50} values of 215 µM and 3.905 µM respectively. Three 24 h treatments (FB_1, allicin and combined FB_1+allicin) were compared to untreated cells for induction of apoptosis and oxidative stress. Luminometry was used to determine cytotoxicity (lactate dehydrogenase assay), caspase activity and mitochondrial toxicity (apoptosis), and quantify intracellular ROS (iROS) and glutathione (GSH) (oxidative stress). Free radical production was estimated by the TBARS and NOS assays respectively, while DNA damage was evaluated using the comet assay. Western blotting confirmed the expression of various antioxidant and apoptotic proteins, and superoxide dismutase 2 (SOD2) transcripts were quantified using qPCR. ATP concentration was increased for all treatments, but mitochondrial toxicity was increased in the allicin treatment. While lipid peroxidation decreased, luminometry results indicate that iROS was increased and was accompanied by a corresponding decrease in SOD2 and catalase protein expression. Depletion of GSH was consistent with increased GPx1, HSP70 and Nrf2 protein expression suggesting the presence

of oxidative stress. SOD2 transcripts were only increased in the allicin treatment. Apoptosis was initiated as indicated by increased caspases 8 and 9, and pro-apoptotic Bax protein expression, but caspase 3/7 was not activated for the FB_1 treatment. However, DNA fragmentation and cPARP were increased for all treatments suggesting that apoptosis was executed. Overall, FB_1 and allicin individually and combined induced oxidative stress by increasing ROS and decreasing antioxidants. Apoptosis was also induced, although in a caspase independent manner in the FB_1 treatment. Overall, allicin did not ameliorate the effects of FB_1 in Hek293 cells.

CHAPTER 1: INTRODUCTION

1.1 Background

Plants form a vital part in the provision of energy to sustain normal metabolic function. However, the plant based foods consumed may contain harmful substances that arise due to contamination of the plant. Notable examples are toxic fungal metabolites such as fumonisin that are not removed by washing, heating or food preparation methods; exposure results in diverse toxicity ranging from immunotoxicity to cancer. Conversely, the organosulphur-containing herbal constituents that are added to enhance the flavour of food during cooking may confer health-benefits when consumed. Onion and garlic are among the plants that contain these useful substances. Garlic is renowned for its potential anti-cancer properties.

Fumonisin B (FB) mycotoxins are produced as secondary metabolites by fungi including *Fusarium verticillioides* (formerly called *Fusarium moniliforme*), *Fusarium proliferatum* and *Aspergillus niger*. They are known to contaminate crops such as maize, wheat and other grain products. Fumonisin B_1 (FB_1) is the most toxic member of the 28 types of the fumonisin family that have been characterised (Miller *et al*., 1993, Berek *et al*., 2001, Schmale and Munkvold, 2009, De Baere *et al*., 2018).

Human and animal exposure to FB_1 occurs via consumption of contaminated maize and other maize products. Exposure to FB_1 produces varying clinical symptoms from species to species and includes pulmonary oedema in pigs, leukoencephalomalacia in horses and oesophageal cancer (OC) in humans (Harrison *et al*., 1990, Kellerman *et al*., 1990, Van der Westhuizen *et al*., 2010). *In vivo* studies suggest the existence of fumonisin-induced carcinogenicity, immunosuppression, hepatotoxicity and nephrotoxicity in laboratory animals (Howard *et al*., 2001, De Baere *et al*., 2018).

When tested, FB_1 is neither genotoxic nor mutagenic according to standard protocols for genotoxic carcinogens, meaning it has no direct mechanism by which it affects DNA (Fink-Grernmels, 1999). The accepted mechanism for FB_1 cytotoxic effects is dysregulation of sphingolipid metabolism, however a study by Chuturgoon *et al.* (2014) has proposed an alternative mechanism of cytotoxicity which involves histone demethylation and DNA hypomethylation (Chuturgoon *et al*., 2014). Furthermore, FB_1 exposure has been shown to induce oxidative stress and thus play a role in carcinogenicity and toxicity. FB_1 was also found to activate apoptosis in many cell lines, primary cell cultures as well as *in vivo (*Domijan, 2012*)*. An epigenetic mechanism of CpG promoter DNA methylation may play a big part in FB_1 toxicity as suggested by a study done on rat kidney and liver cells (Klarić *et al*., 2007, Sancak and Ozden, 2015, Demirel *et al*., 2015).

FB_1 is poorly absorbed and rapidly eliminated, a characteristic that could be attributed to the polar nature of this mycotoxin. Excretion occurs in both faeces and urine. In fact, urinary FB_1 may be used to assess human exposure to FB_1 and suggests ongoing exposure of the urinary system, including the kidney to FB_1. A study by Howard *et al.* (2001) using rats and mice found that FB_1 was a renal carcinogen in male rats' diet at higher dosages (Howard *et al.*, 2001), this finding supported a study that hypothesised that FB_1 can be carcinogenic at increased levels of exposure (Dragan *et al*., 2001). The inhibition of sphingolipid synthesis was accompanied by decreased cell proliferation in pig kidney epithelial cells (LLC-PK_1, renal proximal tubule epithelial cells developed from pigs) following exposure to fumonisins (Abado-Becognee *et al.*, 1998). FB_1 was also found to target the proximal tubular epithelium cells in kidneys of rabbits and presented with toxin-induced renal failure (Gumprecht *et al*., 1995). It is therefore necessary to assess the effect of FB_1 in human kidney cells.

Garlic (*Allium sativum*) is a well-known food additive with many postulated health benefits that are attributed to the compound allicin (*diallyl thiosulfinate*) (Amagase, 2006). However, allicin is not present in garlic cloves; rather this unstable organosulphur compound is liberated when whole garlic

is macerated. Chopping, crushing or chewing garlic results in the release of alliinase, the enzyme responsible for the conversion of alliin to allicin. Allicin is found to have numerous biological effects such as anti-cancer, anti-microbial, anti-viral and anti-bacterial activities. Studies have shown that the anti-cancer properties may be due to inhibition of cancer cell proliferation or induction of apoptosis. In addition, allicin possesses powerful antioxidant properties (Hirsch et al., 2000, Oommen *et al*., 2004).

1.2 Problem statement

Consumption of fungal-contaminated maize, wheat and other grain products has adverse effects in animals and humans. The mycotoxin FB_1 predisposes different species to varying clinical symptoms including OC in humans and kidney cancer in rats. The study done by van der Westhuizen *et al.* (2010) on the prevalence of human OC in Southern Africa due to the exposure to FB_1 necessitates the study on the implication of FB_1 in kidney toxicity (Van der Westhuizen *et al*., 2010). While FB_1 dysregulates apoptosis and induces oxidative stress, allicin induces apoptosis and acts as an antioxidant. Therefore, the potential antagonistic effect of allicin as an inexpensive and implementable preventative measure against FB_1-induced cytotoxicity warrants investigation.

1.3 Hypothesis

FB_1 induced cytotoxicity in human kidney cells may be reduced by co-exposure to allicin.

1.4 Aim

This study aimed to determine the cytotoxic effects of FB_1 in human kidney cells and the ability of allicin to ameliorate these effects.

1.5 Objectives

The objectives are to determine the:

- IC_{50} following exposure to a range of FB_1 and allicin concentrations respectively

- involvement of oxidative stress as a mechanism of FB_1-mediated cytotoxicity, and allicin response to the cytotoxic manifestations
- effect of FB_1, allicin and a combination of FB_1 and allicin exposure on apoptosis induction

CHAPTER 2: LITERATURE REVIEW

2.1 Fumonisin B_1

2.1.1 Background

Fumonisins are mycotoxins produced as secondary by-products of *Fusarium* species (Seefelder *et al*., 2003). *Fusarium verticillioides* (Sacc.) Nirenberg (previously known as *Fusarium moniliforme*) and *Fusarium proliferatum* are two of the most prominent *Fusarium* species that produce fumonisins. Due to their geographical distribution and high production levels (Abuja and Albertini, 2001), these contaminating species make fumonisin a worldwide contaminant of maize, a dietary staple for human food and animal feed (Hendricks, 1999, Hassan *et al*., 2015).

Twenty eight types of fumonisins have been discovered and characterised into 4 groups namely, fumonisin A, B, C and P (FA, FB, FC and FP series) (Abuja and Albertini, 2001). The FB series is the most common of all the fumonisins and within it, FB_1 is the most notorious in prevalence and toxicity.

2.1.2 Structural composition

FB_1 (Figure 2.1) is composed of two units of propane-1, 2, 3-tricarboxylic acid (TCA) that is esterified to a 2S-amino-12S,16R-dimethyl-3S,5R,10R,14S,15R-pentahydroxy-eicosane backbone by a diester bridge at the C-14 and C-15 hydroxy groups. The presence of the four free carboxyl groups, the hydroxyl groups and the amino group make FB_1 soluble in polar solvents and insoluble in some organic solvents (Chu *et al*., 2012).

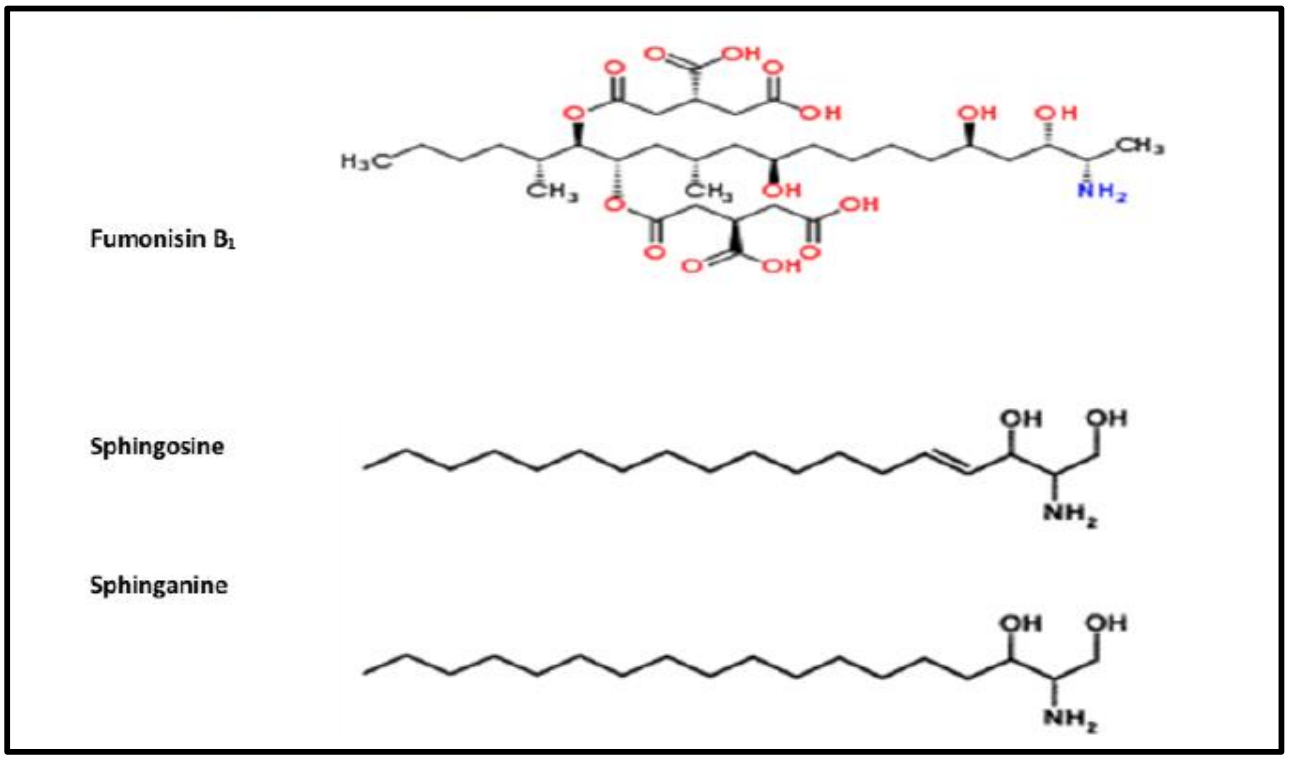

Figure 2.1 : Structure of FB_1 showing its similarities to sphinganine and sphingosine (Humpf and Voss, 2004).

2.1.3 Mechanism of action

Fumonisin B_1 is similar in structure to the bioactive lipid signaling molecules, sphingolipids (Figure 2.1). Sphingolipid biosynthesis is a *de novo* pathway set off by the condensation of serine and palmitoyl-CoA catalysed by serine palmitoyl transferase to form 3-keto-dihydrosphingosine. 3-keto-dihydrosphingosine is then reduced to sphinganine (dihydrosphingosine). The sphinganine is subsequently N-acylated by dihydroceramide synthases to generate dihydroceramide which is desaturated creating a 4, 5-trans-double bond to form ceramide. This pathway produces and culminates in the production of bioactive intermediates comprising sphingosine, dihydroceramide and ceramide (Wang *et al*., 1991, Merrill, 2002).

A study by Wang *et al*. (1991) found that fumonisins could disrupt the *de novo* metabolism of sphingolipids (Figure 2.2) via the inhibition of ceramide synthase (Wang *et al*., 1991). The consequence of FB_1-induced inhibition of ceramide synthase *in vivo* is the accumulation of sphinganine, an occasional increase of sphingosine, high sphinganine/sphingosine ratio,

accumulation of 1-phosphate metabolites of sphinganine and sphingosine and low complex sphingolipids (Voss and Riley, 2013). These changes represent an important step in fumonisin toxicity that sets off a series of reactions which disrupt cell growth, differentiation and cell injury *in vitro* and *in vivo*.

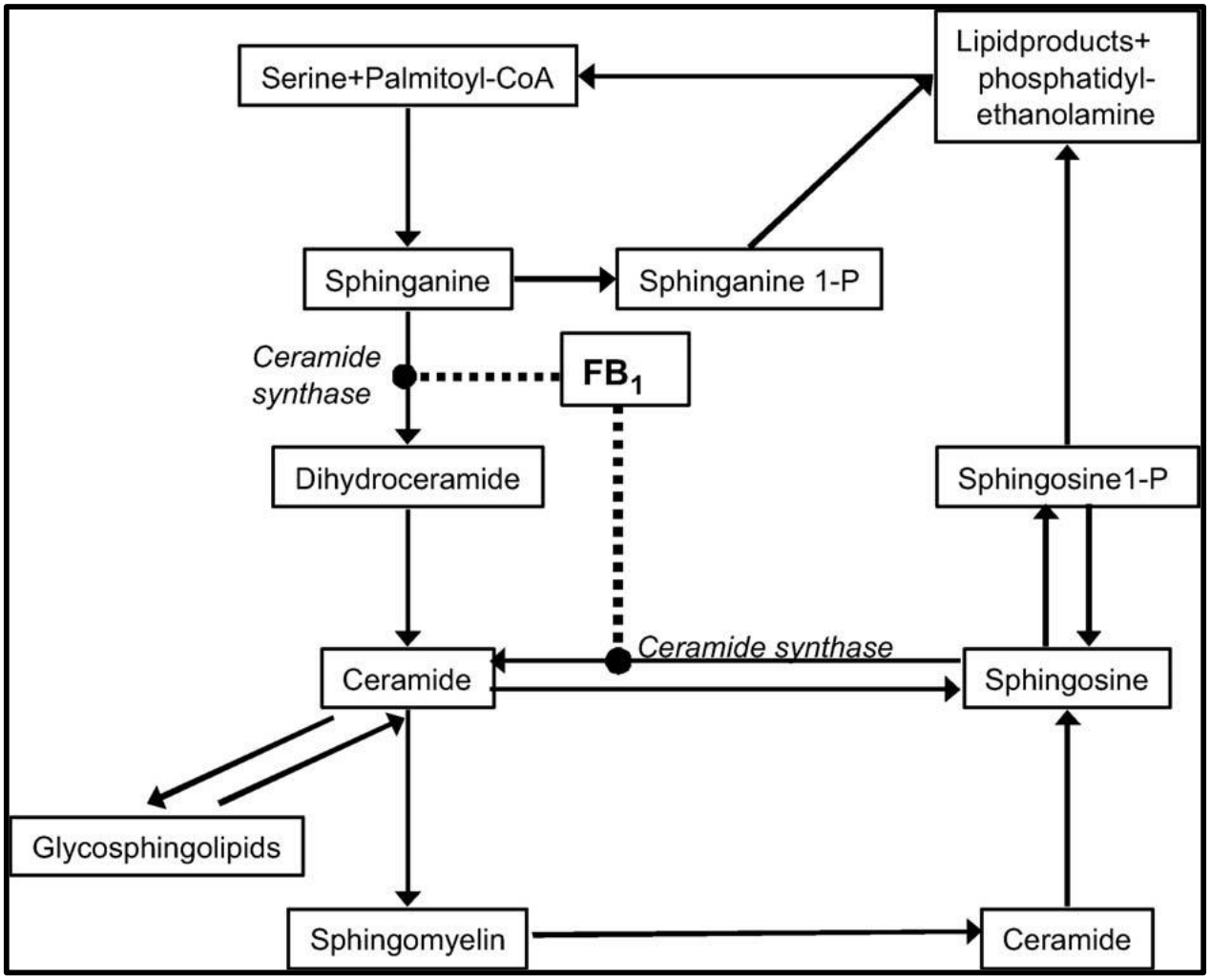

Figure 2.2 : Schematic representation of sphingolipid biosynthesis in animal cells and the points at which FB_1 inhibits ceramide synthase (Merrill Jr *et al.*, 2001, Stockmann-Juvala and Savolainen, 2008).

An alternative mechanism of action was recently described in a study by Chuturgoon *et al.* (2014). this study associated FB_1 with DNA methylation, a major epigenetic modification (Chuturgoon *et al.*, 2014).

2.1.4 Epigenetics

Epigenetic modifications are heritable changes in gene activity or function that are not encoded by the DNA sequence. Major components of epigenetic modification include DNA methylation, histone modification and microRNAs (miRNAs) which contribute to gene expression through altering the chromatin structure and DNA accessibility. DNA methylation and histone modification exert their actions at the transcriptional level and miRNAs at the post-transcriptional level (Baccarelli and Bollati, 2009, Halušková, 2010, Sharma *et al*., 2010).

2.1.5 Effects of fumonisin B_1 in animals

The effects of FB_1 exposure have continuously proven to vary in different species (Stockmann-Juvala and Savolainen, 2008, Chuturgoon *et al*., 2014). Reports have shown FB_1 to induce leukoencephalomalacia (LEM) in horses (Marasas *et al*., 1988, Kellerman *et al*., 1990, Marasas *et al*., 2014), pulmonary oedema in swine (Harrison *et al*., 1990) and OC in humans (Sydenham *et al*., 1990, Rheeder *et al*., 1992, Yoshizawa *et al*., 1994, Sun *et al*., 2007) FB_1 is also renowned for its nephrotoxic, hepatotoxic and neurotoxic effects in laboratory animals (Riley *et al*., 1994, Voss *et al*., 1995, Gelderblom *et al*., 2001, Marasas *et al*., 2004).

The presence of FB_1 in maize and wheat products intended for human consumption has been linked to human health risks including OC and neural tube defects (NTD). OC has been epidemiologically linked to FB_1 contaminated maize in studies done in South Africa where reports showed that a high risk of OC development was proportional to an increased intake of maize (Marasas and WFO, 1988).

Neural tube defects are congenital malformations of the brain and spinal cord that occur when the embryonic neural tube fails to close. This common birth defect has been associated with high exposure of FB_1 in areas known to have high consumption of maize. A hypothesis for this association stated that FB_1-induced inhibition of ceramide synthase that disrupts sphingolipid biosynthesis and

subsequently folate transport causes a decrease in folate uptake that increases the risk of NTD (Hendricks, 1999, Marasas *et al*., 2004, Missmer *et al*., 2005, Stockmann-Juvala and Savolainen, 2008).

Many studies have been done on the effects of FB_1 toxicity in animals, commonly laboratory animals. These effects include hepatotoxicity, nephrotoxicity, immunotoxicity, neurotoxicity and pulmonotoxicity. Studies have demonstrated the occurrence of FB_1-induced hepatotoxicity and nephrotoxicity in laboratory animals through repeated exposure. Gelderblom *et al.* (1988) found that male BD IX rats developed chronic toxic hepatosis when treated with 48 mgFB_1/kg body weight daily (12 days) then 70 mgFB_1/kg body weight daily (9 days) in a 21-day experiment (Gelderblom *et al*., 1988). In a study by Voss *et al.* (1993) both hepatotoxicity and nephrotoxicity were demonstrated in a study done on Sprague-Dawley rats (Voss *et al*., 1993). FB_1-induced toxicity in the liver and kidneys is a common consequence of various feeding studies (Voss *et al*., 1993, Riley *et al*., 1994, Howard *et al*., 2001).

The immunological effects of FB_1 have only been studied based on the cytokine profile of different cell types and organs. A study on Sprague-Dawley rats demonstrated that FB_1 affected the humoral immune response of the male rats (Tryphonas *et al*., 1997). The most common neurotoxic effect of FB_1, LEM developed through oral or intravenous administration was found in horses (Kellerman *et al*., 1990).

FB_1 has been shown to exhibit carcinogenic effects on various cells in animals and humans. The International Agency for Research on Cancer (IARC) has classified FB_1 as a type 2B carcinogen, a possible human carcinogen. A 2-year study by Howard *et al.* (2001) found FB_1 to be a renal carcinogen causing renal tubule tumours in male F344 rats at doses 50 and 150 ppm and a hepatocarcinogen inducing hepatocellular adenomas and carcinomas in female $B6C3F_1$ mice at doses

50 and 80 ppm (Howard *et al*., 2001). In rat kidney epithelial cells, FB_1 was reported to have altered global histone modification (Sancak and Ozden, 2015) and in human hepatoma cells, found to have induced global DNA methylation (Chuturgoon *et al*., 2014) which may be linked to the progression of cancer, tumourigenesis or cell cycle arrest.

2.1.6 Molecular effects of FB_1 exposure

The two main consequences of FB_1 exposure are oxidative stress and apoptosis. Together, these processes are responsible for the diverse effects associated with FB_1 exposure.

2.1.6.1 Oxidative Stress

Reactive oxygen species (ROS) are by-products of aerobic respiration in the process of normal cellular metabolism (Held, 2012). Oxygen is converted through a series of reduction reactions to superoxide (O_2^-), hydrogen peroxide (H_2O_2) and water (H_2O) (Figure 2.3). These radical oxygen species are counteracted by an arsenal of antioxidant proteins or enzymes. Superoxide dismutases (SODs) are known to be the major antioxidant defense proteins, catalysing the conversion of O_2^- into H_2O_2 – in the mitochondria, SOD2 (MnSOD) is the isoform responsible for this reaction. The resulting H_2O_2 is further converted to H_2O, catalysed by glutathione peroxidase (GPx), catalase or peroxiredoxin (Prxs) (Figure 2.3). GPx simultaneously catalyses the formation of oxidised glutathione (GSSG) from reduced glutathione (GSH) (Figure 2.3) (Halliwell, 2007, Gupta *et al*., 2014). Glutathione is an important antioxidant vastly populated in the liver and is needed by the kidneys to maintain homeostasis, making it crucial for the body's detoxification process (Lash, 2005, Zitka *et al*., 2012). Reduced GSH is a ROS scavenger. On DNA and other biomolecules it demolishes oxygen free radicals, radical centers and reactive hydroxyl free radicals (Mytilineou *et al*., 2002). The relative concentration of these antioxidants is controlled by the nuclear factor erythroid 2 (NFE2)-related factor 2 (Nrf2) (Fukai and Ushio-Fukai, 2011), a transcription factor that exerts cytoprotective properties against oxidative stress.

Intracellular and/or extracellular ROS are essential for biochemical processes such as cellular function, intracellular signaling and defense against microorganisms at low levels (Fukai and Ushio-Fukai, 2011). However, at increased levels ROS inactivate or deplete antioxidant enzymes (Lushchak, 2015), resulting in an accumulation or inadequate removal of ROS and oxidative stress (Fukai and Ushio-Fukai, 2011). Oxidative stress therefore is increased toxic levels of ROS production surpassing the cell's ability to counteract the effects. The induction of oxidative stress not only damages tissues, but causes genetic instability and disrupts normal cellular functioning (Towner *et al*., 2003, Mehta *et al*., 2007, Matur *et al*., 2011, Abbes *et al*., 2016, Khan *et al*., 2018b).

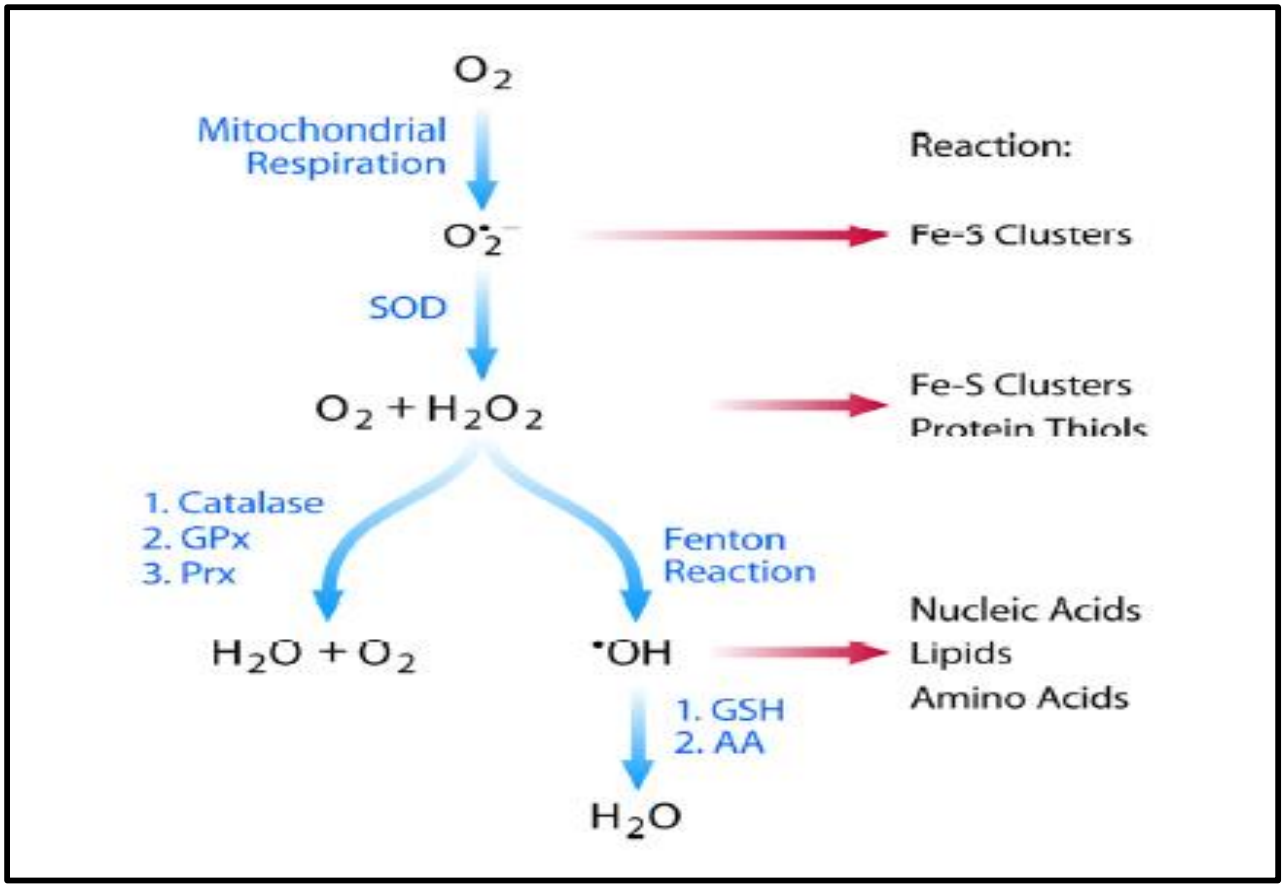

Figure 2.3 : Schematic representation of the synthesis and detoxification of ROS (Merksamer *et al*., 2013).

FB_1-induced oxidative stress varies from cell type to host species, demonstrated by studies done on OC cells, mice, hens, humans and rats (Towner *et al*., 2003, Mehta *et al*., 2007, Matur *et al*., 2011, Abbes *et al*., 2016, Khan *et al*., 2018b). In humans, it is postulated that oxidative stress mediates the

immunotoxic effects of FB_1 (Stockmann-Juvala *et al.*, 2007, Klaric *et al*., 2008, Domijan *et al*., 2012). The findings of a study by Abbes *et al.* (2016) further verified the role of FB_1 in inducing oxidative stress by demonstrating increased levels of oxidative stress markers in mice spleen where ROS production was increased overall. It hypothesised that genotoxicity or mutagenicity may be indirect consequences of FB_1-induced oxidative damage (Hassan *et al*., 2015, Abbes *et al*., 2016). It must also be noted that cells may respond to oxidative stress by triggering apoptosis.

2.1.6.2 Apoptosis

The regulation of homeostasis and other cellular processes helps maintain cellular functionality. Apoptosis is a biological process of programmed cell death marked by cell shrinkage, DNA fragmentation and chromatin condensation that occurs as a mechanism of defense that removes damaged cells (Kerr *et al*., 1972, Renehan *et al*., 2001). This process is controlled by caspases, which are initially produced as inactive pre-enzymes (procaspases) before activation through different cleavage processes at specific aspartate residues (Shi, 2004, Elmore, 2007).

Apoptosis occurs via the intrinsic and extrinsic pathways (Figure 2.4). The intrinsic pathway is triggered by a number of mitochondrial stimuli such as DNA damage, oxidative stress and growth factor deprivation. These stimuli produce signals intracellularly mediated by the mitochondria. The extrinsic pathway is activated through the binding of death receptors to ligands to transmit apoptotic signals (Elmore, 2007, Mukhopadhyay *et al*., 2014).

The intrinsic pathway, also known as the mitochondrial pathway is mainly regulated by the Bcl-2 family proteins responsible for mitochondrial membrane permeability (Figure 2.4). They stimulate BH3 family proteins that activate BAX and BAK pro-apoptotic effectors. The process is triggered by several stimulating factors that disturb the electrochemical gradient, increase membrane permeability

and release apoptogenic factors. A disturbance in the mitochondrial membrane integrity results in either necrosis and/or the release of cytochrome *c* into the cytosol which activates initiator caspase 9 through the assembly of an apoptosome (a multiprotein caspase-activating complex comprised of Apaf1 and procaspase 9) that activates effector caspases 3/7 that function to execute apoptosis (Hassan *et al*., 2014, Baig *et al*., 2017).

The death receptor-mediated pathway is triggered when the signaling mechanism of death domain (DD)-containing tumour necrosis factor (TNF) family receptors activates caspases (Figure 2.4). Death receptor ligands bind to the plasma membrane forming a death-inducing signaling complex (DISC) to activate procaspases 8 and 10. Caspase 8 which contains death effector domains on the N-terminal prodomains initiates proapoptotic cascade of caspases. Caspase 8 can either activate the intrinsic pathway through the activation of tBID which triggers the oligomerisation of Bak to release cytochrome c or activates caspase 3 (Figure 2.4). Caspase 3 cleaves inhibitor of caspase activated DNase (iCAD) to CAD that leads to DNA fragmentation, apoptotic blebs, apoptotic bodies and chromatin condensation (Hassan *et al*., 2014, Koff *et al*., 2015).

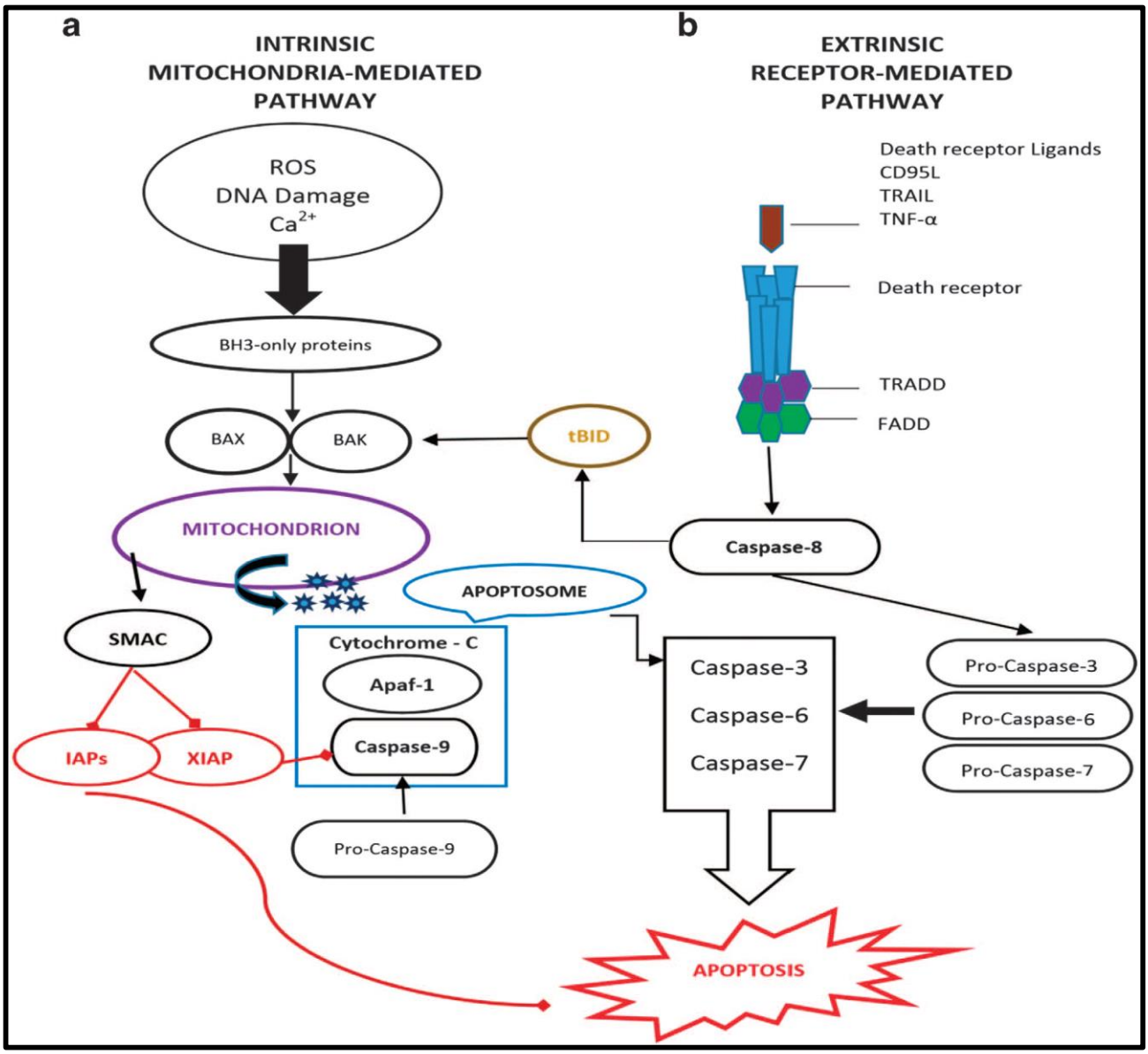

Figure 2.4: Intrinsic and extrinsic pathways of apoptosis (Baig *et al*., 2017).

Exposure to FB_1 results in organ-specific toxic manifestations. Likewise, the induction of apoptosis by FB_1 is dependent on cell type and species, as well as the concentration (Khan *et al*., 2018). For example, neuroblastoma cells are sensitive to FB_1-induced apoptosis (Stockman-Juvala, 2006), while apoptosis is inhibited in HepG2 cells (Chuturgoon *et al*., 2015). A number of animal studies investigating the consequences of FB_1 exposure describe one of its effects to be apoptosis. This effect results from FB_1-induced disruption of sphingolipid metabolism by inhibiting the enzyme ceramide synthase (Wang *et al*., 1991, Brenner and Kroemer, 2000, Minervini *et al*., 2004). Dragan *et al*. (2001) characterised FB_1-induced apoptosis as mechanism of action in carcinogenesis (Dragan *et al*., 2001).

2.2 Medicinal plants

Plants have been used for medicinal purposes for many years. Scientific research as shown their health benefits to span from antiseptic properties to the treatment of cancer (Greenwell and Rahman, 2015). Their wide array of health benefits has since prompted the identification of plant species and their extracts for the development of some therapeutic drugs. Among many, *Allium sativum* and its constituents is one of the most commonly studied plants for its potential to alleviate and prevent disease (Amagase, 2006, Iciek *et al*., 2009).

2.2.1 *Allium sativum*

Allium sativum, more commonly known as garlic, is a medicinal plant whose use in different cultures has had many beneficial health effects through history. Its biological benefits include anti-cancer properties, enhanced immune function, reduced cardiovascular disease risk factors, anti-bacterial, anti-fungal and anti-parasitic properties among many (Mikaili *et al*., 2013, Gruhlke *et al*., 2016). The varying effects of garlic have been attributed to its different preparations under four categories namely garlic oil, aged garlic extract (AGE), garlic powder and garlic oil macerate. A common characteristic of garlic is its distinct smell caused by oil-soluble sulfur constituents; whole intact garlic comprises primary sulfur-containing molecules which include γ-glutamyl-*S*-alk(en)yl-L-cysteines and *S*-alk-(en)yl-L-cysteine sulfoxides (i.e alliin) (Bhandari, 2012)

2.2.2 Allicin, an organosulphur compound from garlic

When the plant tissue is damaged or whole garlic is macerated, garlic compounds undergo rapid conversion into organosulphur compounds such as allicin (alkyl alkane-thiosulfinate) which represents the biologically active component of crushed garlic. Allicin is synthesised via a two-step reaction that begins when the enzyme alliinase that hydrolyses alliin within the cytosol to produce dehydroalanine and odiferous sulfenic acid (Bat-Chen *et al*., 2010). A spontaneous condensation reaction of two allyl sulfenic molecules (2-propenesulfenic acid) occur forming one allicin molecule

(Figure 2.5). Allicin may then be degraded to ajoene by heating, or condense with other allicin molecules yielding secondary products including diallyl sulfide (DAS), diallyl disulfide (DADS) and diallyl trisulfide (DAT) and dithiins (Figure 2.5). In a different pathway, γ-glutamyl-cysteines are converted to S-allylcysteine (SAC) (Mikaili *et al*., 2013, Luo *et al*., 2016).

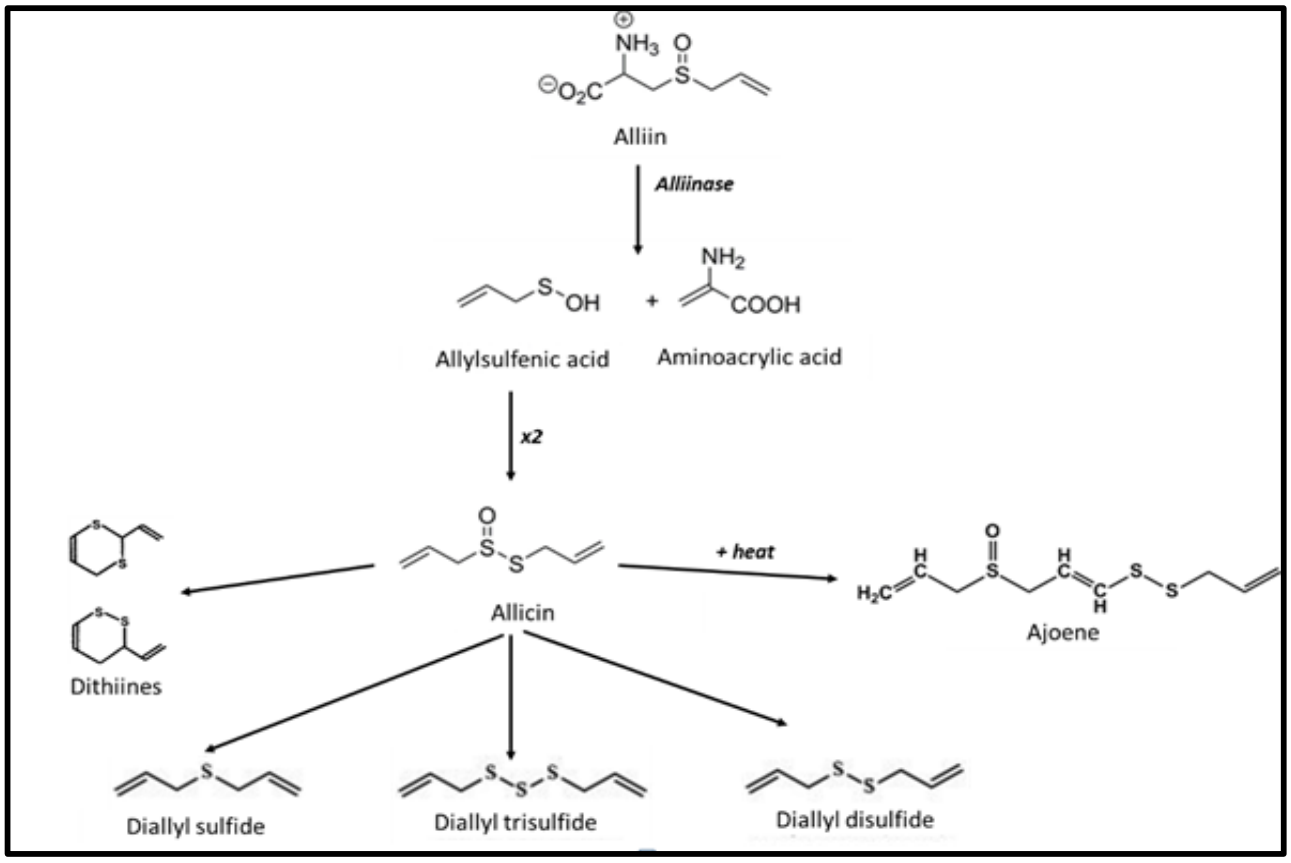

Figure 2.5: The two-step biosynthesis of allicin involves the enzymatic conversion of alliin to 2-propenosulfenic acid, and subsequent condensation to allicin. Secondary products are formed by various meansof. Adapted from (Gruhlke *et al*., 2016, Luo *et al*., 2016).

2.2.3 Effects of allicin

Allicin has been vastly studied for its many health benefits including anti-cancer activity through allicin-induced apoptosis and inhibition of cancer cell proliferation in different cell lines (Siegers *et al*., 1999, Hirsch *et al*., 2000, Bat-Chen *et al*., 2010). Allicin-induced apoptosis varied in different cell lines, and was found to be both caspase-dependent (Oommen *et al*., 2004, Bat-Chen *et al*., 2010) and caspase-independent (Park *et al*., 2005) . It has been suggested that inhibition of cell proliferation

mediated by allicin may be associated with modulation of tubulin, which interferes with mitotic spindle formation and cell division (Prager-Khoutorsky *et al*., 2007).

The exact mechanisms by which allicin induces its antioxidant effects remains unclear. However, studies have shown it to have free radical scavenging effects, ability to inhibit the production of O_2^- and react with thiol-containing compounds. This reactive sulfur species also has the ability to oxidise GSH and cysteine residues in various proteins because of its membrane permeability. Studies have also shown that in the presence of ROS, allicin induces phase II detoxification and upregulates nuclear factor erythroid-related factor 2 (Nrf2), thereby fulfilling an essential role in the replenishment of several antioxidants, including SOD2 and GSH (Gruhlke *et al*., 2016).

CHAPTER 3: MATERIALS AND METHODS

3.1 Materials

FB_1 was purchased from Sigma Aldrich (Johannesburg, South Africa (SA)). The human embryonic kidney (Hek293) cells were purchased from Highveld Biological (Johannesburg, SA). Cell culture reagents were acquired from Whitehead Scientific (Johannesburg, SA). Western blotting reagents were purchased from Bio-Rad (Hercules, CA). Antibodies and Promega kits were bought from Anatech (Johannesburg, SA). Other reagents were obtained from Merck (Darmstadt, Germany).

3.2 FB_1 and allicin preparation

Stock solutions of FB_1 (1468.5 µM) and allicin (1848.8 µM) were prepared in 0.1 M phosphate buffered saline (PBS, pH 7.4). These stocks were stored at 4 ^{o}C and diluted for subsequent assays.

3.3 Cell culture

The Hek293cell line was reconstituted by transferring a vial of cryopreserved cells into a sterile 25 cm^3 cell culture flask containing 10 ml of complete culture medium (CCM) comprising of Dulbecco's Modified Eagle's Medium (DMEM) supplemented with 10 % foetal calf serum, 25 mM HEPES, 1 % L-glutamine and 1 % penicillin-streptomycin-fungizone. The flask was incubated for 4 hours (4 h) at 37 °C, in a 5 % CO_2-supplemented incubator, after which the CCM was discarded and replaced with 5 ml of fresh CCM. Cells were maintained until 90 % confluence was reached. Confluent flasks were washed with phosphate-buffered saline (PBS); the cells were dislodged and counted (150 µl of CCM, 50 µl of trypan blue, 50 µl of cell suspension in an eppendorf and transferring 10 µl of this mixture onto a haemocytometer) for sub-culturing or storage.

3.4 Methylthiazol tetrazolium (MTT) Assay

3.4.1 Principle

The methylthiazol tetrazolium (MTT) assay was used to measure cell viability and cytotoxicity in Hek293 cells following exposure to FB_1 and allicin respectively. The yellow MTT salt that crosses the membranes of living cells is reduced to a purple formazan product by mitochondrial succinate dehydrogenase (SDH) (Figure 3.1) and therefore reflects the number of viable cells (Abate *et al*., 1998). The MTT assay generates a half maximum inhibitory concentration (IC_{50}) that refers to a concentration that inhibits a population's biochemical functioning by 50 %. The IC_{50} will be used as the treatment dose in subsequent assays.

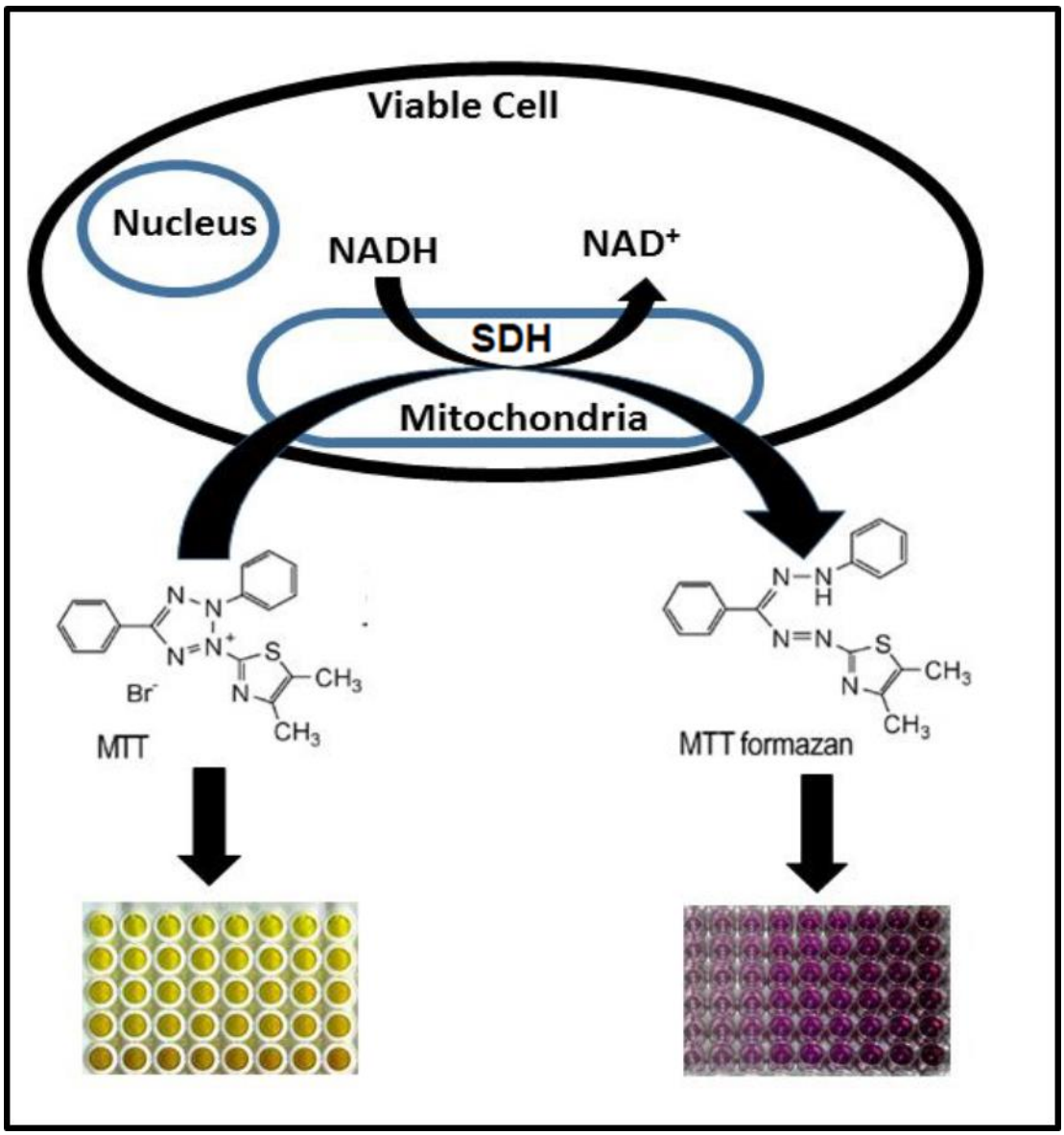

Figure 3.1 : Metabolic cellular reduction of yellow MTT salt into a purple formazan (Riss *et al*., 2004).

3.4.2 Protocol

The Hek293 cells were seeded into a 96-well microtitre plate at a density of 15,000 cells/well (200 µl) in triplicate and allowed to attach overnight. Cells were incubated with a range of FB_1 and allicin concentrations (0-1000 µM) at 37 °C for 24 h. Thereafter, the cells were incubated with 20 µl MTT salt solution (5 mg/ml in 0.1 M PBS) and 100 µl CCM at 37 °C. After 4 h incubation, the MTT salt was discarded and replaced with 100 µl of DMSO for the solubilisation of formazan crystals and further incubated for an hour at 37 ^{0}C. The optical density of the samples was read at 570 nm and 690 nm using the Bio-Tek µQuant spectrophotometer (USA). The cell viability and the concentration dependent response curve were plotted using GraphPad Prism v5.0 software and an IC_{50} was generated.

Flasks of Hek293 cells were grown to confluence and treated as follows:

- control - CCM only
- IC_{50} of FB_1
- IC_{50} of allicin and
- Combined IC_{50} of FB_1 + IC_{50} of allicin

After 24 h treatment, the cells were washed, resuspended in PBS, counted and the cell number was adjusted for use in subsequent assays.

3.5 Bioluminescence Assays

Bioluminescence is the generation and emission of light by an organism due to a chemical reaction whereby chemical energy is transformed into light energy and the outcome is chemiluminescence (Hastings, 1968). The assay is based on the luciferin-luciferase reaction that occurs in the firefly. Luciferase is the enzyme that catalyses the monooxygenation of D-luciferin in the presence of magnesium, ATP and oxygen, producing inactive oxyluciferin. The intensity of light that is produced

by this reaction is directly proportional to the concentration of the substrate being measured (Lundin, 2000).

3.5.1 CytoTox-ONE™ Homogenous Membrane Integrity Assay

3.5.1.1 Principle

While the MTT assay was used to estimate the number of viable cells, studies have shown that it is invaluable to measure the leakage of cytoplasmic components into the surrounding culture medium in order to quantify non-viable cells. This assay quantifies the fluorescent signal generated by resofurin when lactate dehydrogenase (LDH) released from cells with damaged membranes into the culture medium participates in a coupled reaction that results in the conversion of resazurin to resofurin (Figure 3.2) (Ronken, 2009).

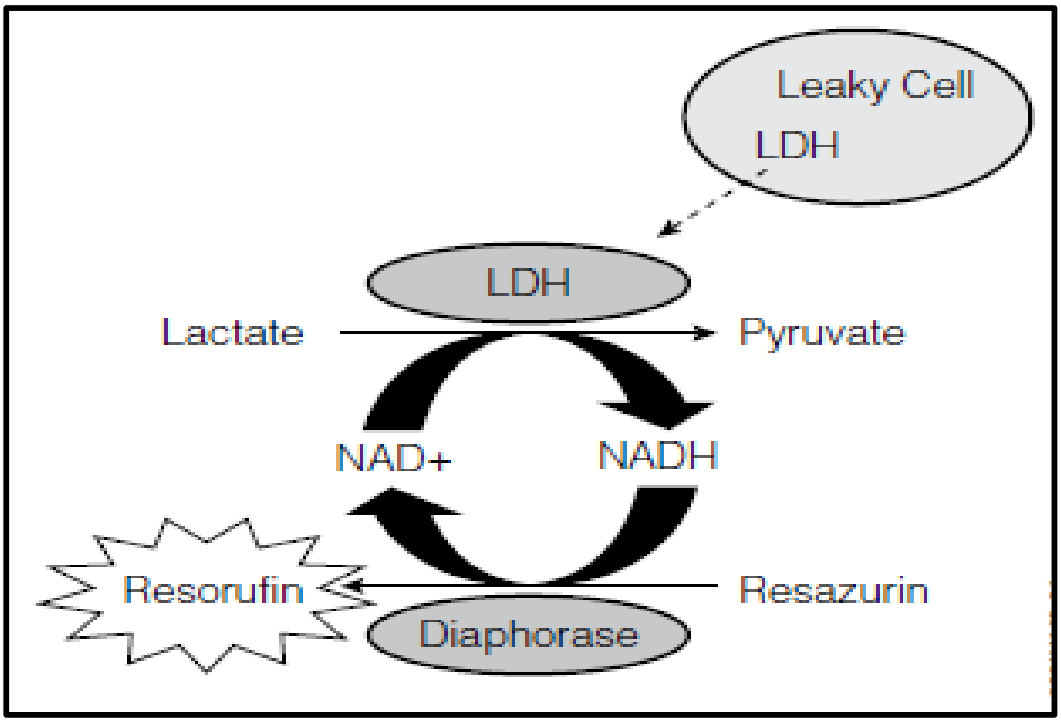

Figure 3.2 : Leakage of LDH from a cell with a damaged membrane (Ronken, 2009).

3.5.1.2 Protocol

The protocol was followed according to the manufacturer's instructions. Briefly, treated Hek293 cells (2×10^4 cells in 100 µl of treatment medium) were transferred to a 96-well white microtitre plate in triplicate and equilibrated to room temperature (RT). Lysis solution was added to all the wells (2 µl).

Thereafter, 100 µl of Promega CytoTox-ONE™ Reagent (#G7890) was aliquoted into all the wells and mixed well before incubation of 10 min at RT. Subsequently, 100 µl of stop solution was added into each well and the microtitre plate was put on the shaker for 10 sec. The fluorescence was obtained using the Promega GloMax®-Multi+ Detection Plate Reader (Turner Bio-systems, Sunnyvale, USA) with an excitation wavelength of 560 nm and an emission wavelength of 590 nm.

$$\%\ \text{cytotoxicity} = 100\ \text{x}\ \frac{(\text{experimental} - \text{culture medium background})}{(\text{max LDH release} - \text{culture medium background})}$$

3.5.2 Caspases

3.5.2.1 Principle

The main workers of apoptosis are a family of proteins called caspases. These are cysteine-aspartate proteases that are involved in the initiation and execution of apoptosis (Garrido and Kroemer, 2004). The caspase activity is based on cleavage of the caspase-luciferin substrate by luciferase. This reaction produces light which is directly proportional to caspase activity (Figure 3.3).

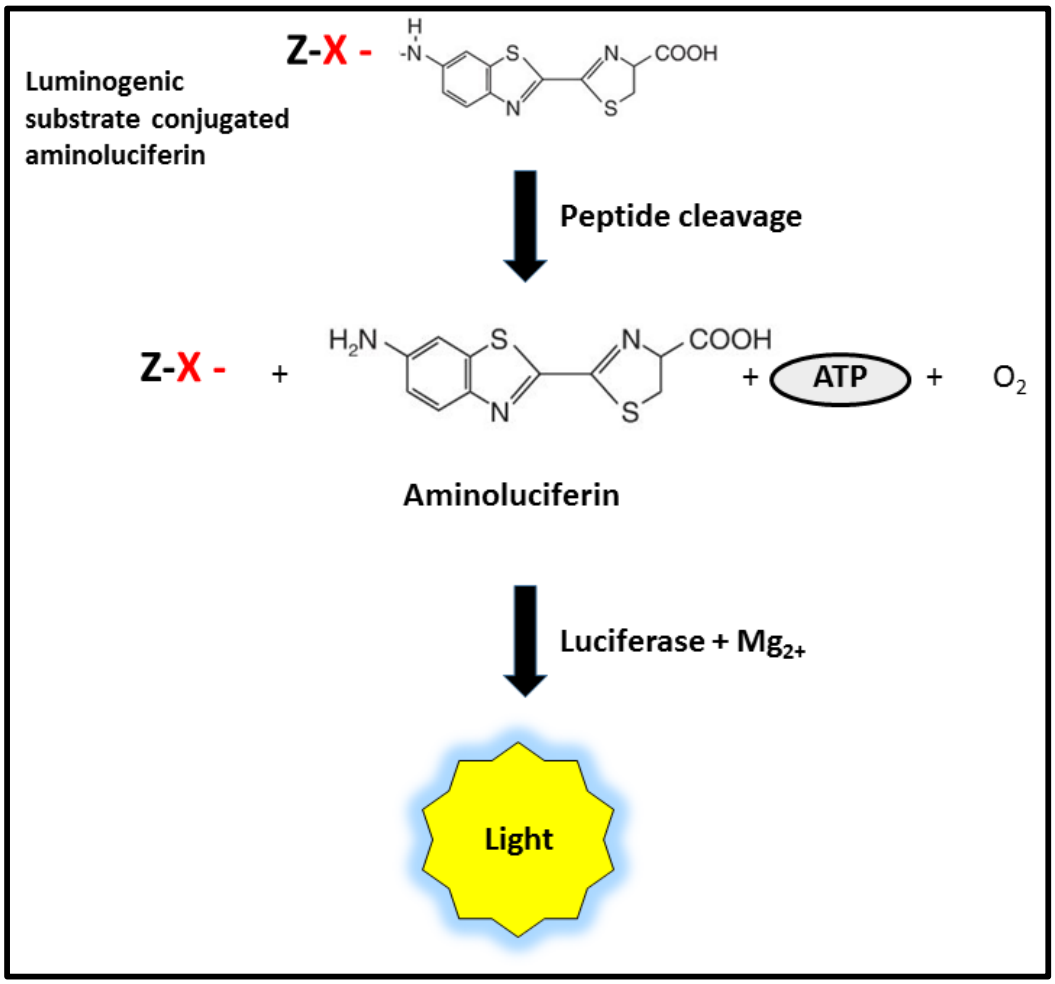

Figure 3.3 : Luminometric measure of caspases 3/7, 8 and 9 activities [Adapted from (Riss *et al.*, 2004, Brunelle and Zhang, 2010, Shunmugam, 2016)].

3.5.2.2 Protocol

The activities of caspase 3/7, 8 and 9 were detected with the Promega Caspase-Glo® assay (#G8091, # G8201 and #G8211 respectively). Briefly, 50 µl of cell suspension (20,000 cells/well in 50 µl 0.1 M PBS) were seeded into duplicate wells of a white, opaque 96-well microtitre plate. As per manufacturer's guidelines, caspase-Glo®-3/7 reagent was reconstituted and 50 µl was added into each well. Thereafter, the plate was incubated in the dark (30 min, RT). The procedure was completed in a similar fashion for caspase 8 and caspase 9. Luminescence was detected using a Modulus™ microplate luminometer (Turner Bio-systems, Sunnyvale, USA) as relative light units (RLU).

3.5.3 CellTiter-Glo® Luminescent Cell Viability Assay

3.5.3.1 Principle

ATP is the universal energy transducer in mammalian cells produced during cellular respiration. Levels of intracellular ATP are a useful indicator of respiratory capacity and mitochondrial function. The assay uses bioluminescence to determine intracellular ATP levels to indicate the number of viable cells in culture. During this reaction, cellular ATP is used in the luciferase reaction to generate a light signal (Figure 3.4). The intensity of light that is produced by this reaction is directly proportional to the concentration of intracellular ATP (Lundin, 2000).

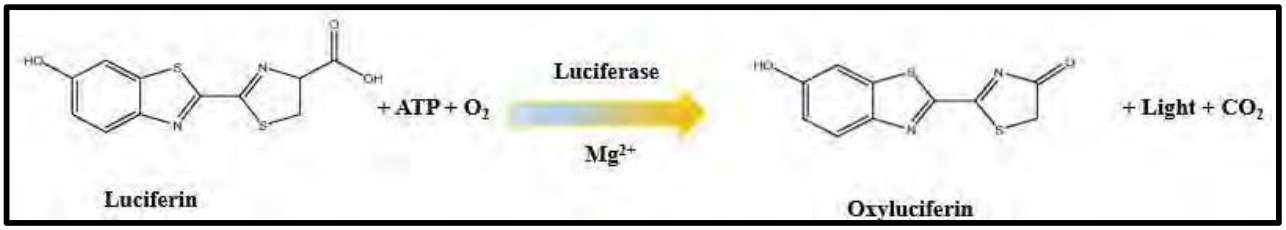

Figure 3.4 : ATP-dependant oxidation of D-luciferin to produce light (Govender, 2016).

3.5.3.2 Protocol

The ATP inside the cells was quantified using the Promega CellTitre-Glo® Assay (#G7570), whereby 50 µl of cell suspension (20,000 cells/well in 50 µl 0.1M PBS) was plated into a 96-well luminometer plate in duplicate. Thereafter, 50 µl of reconstituted CellTiter-Glo® substrate was added in each well. The plate was incubated in the dark for 30 min at RT. The amount of light produced was quantified using the Modulus™ microplate luminometer (Turner Bio-systems, Sunnyvale, USA) and expressed in RLU.

3.5.4 Mitochondrial Toxicity Assay

3.5.4.1 Principle

The Promega Mitochondrial ToxGlo™ Assay (#G8000) serves to predict the integrity of the mitochondria and cellular ATP levels by looking at specific biomarkers that correspond with the normal functioning and state of the mitochondria. This assay achieves such by measuring protease

activity that shows cell membrane integrity and measures ATP levels through a luminescent signal (Figure 3.5).

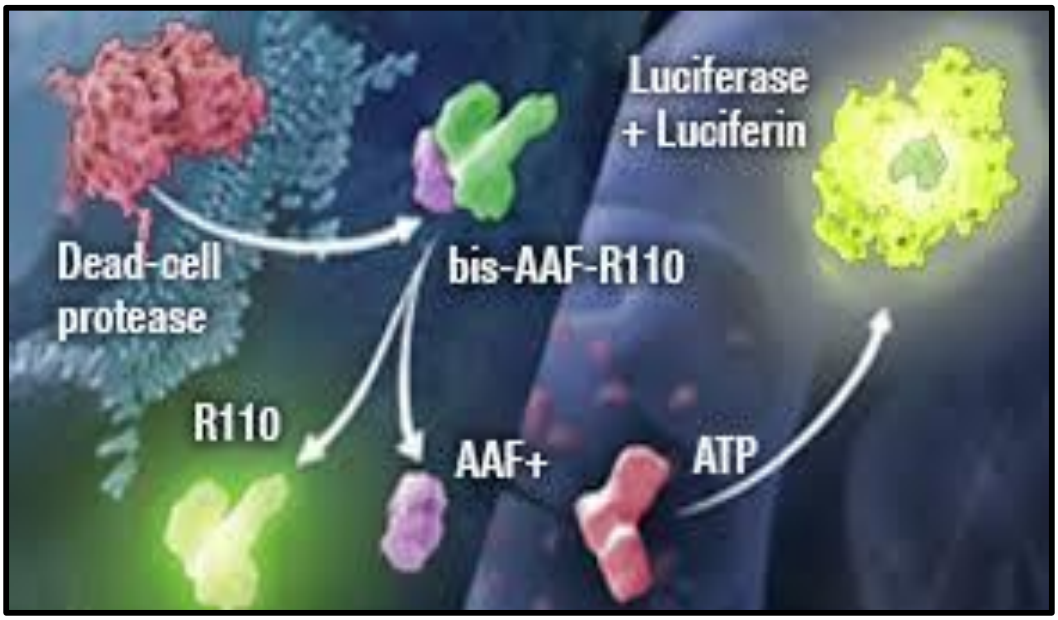

Figure 3.5 : Luminometric measurement of protease activity and ATP in the mitochondria (PT. Indolab utama protocols).

3.5.4.2 Protocol

To a white 96-well microtitre plate, 50 µl of Hek293 cell suspension (20,000 cells) was added into each well and the cells were allowed to attach overnight at 37 ^{o}C (5 % CO_2). Cells were treated in duplicates for 24 h; then 20 µl of 5X cytotoxicity reagent was added into each well, mixed then incubated for 30 min at 37 ^{0}C. Fluorescence was then measured at 485 nm_{Ex}/520–530 nm_{Em}. The assay plate was then equilibrated to room temperature for 10 min before the addition of 100 µl ATP Detection Reagent to each well and mixed for 5 min. The luminescence was then measured after 1 hr.

3.5.5 Ros-Glo H_2O_2 Assay

3.5.5.1 Principle

ROS are generated from the normal metabolic processes that occur in our body. The overproduction of ROS leads to oxidative stress that causes DNA and protein damage as well as lipid peroxidation.

The O_2^- is the most common source of ROS. Superoxide is converted to H_2O_2 by SOD. This assay serves to measure the amount of H_2O_2 by coupling it in a luciferase reaction where the light produced is quantified (Figure 3.6). It also directly links the amount of H_2O_2 to O_2^- production.

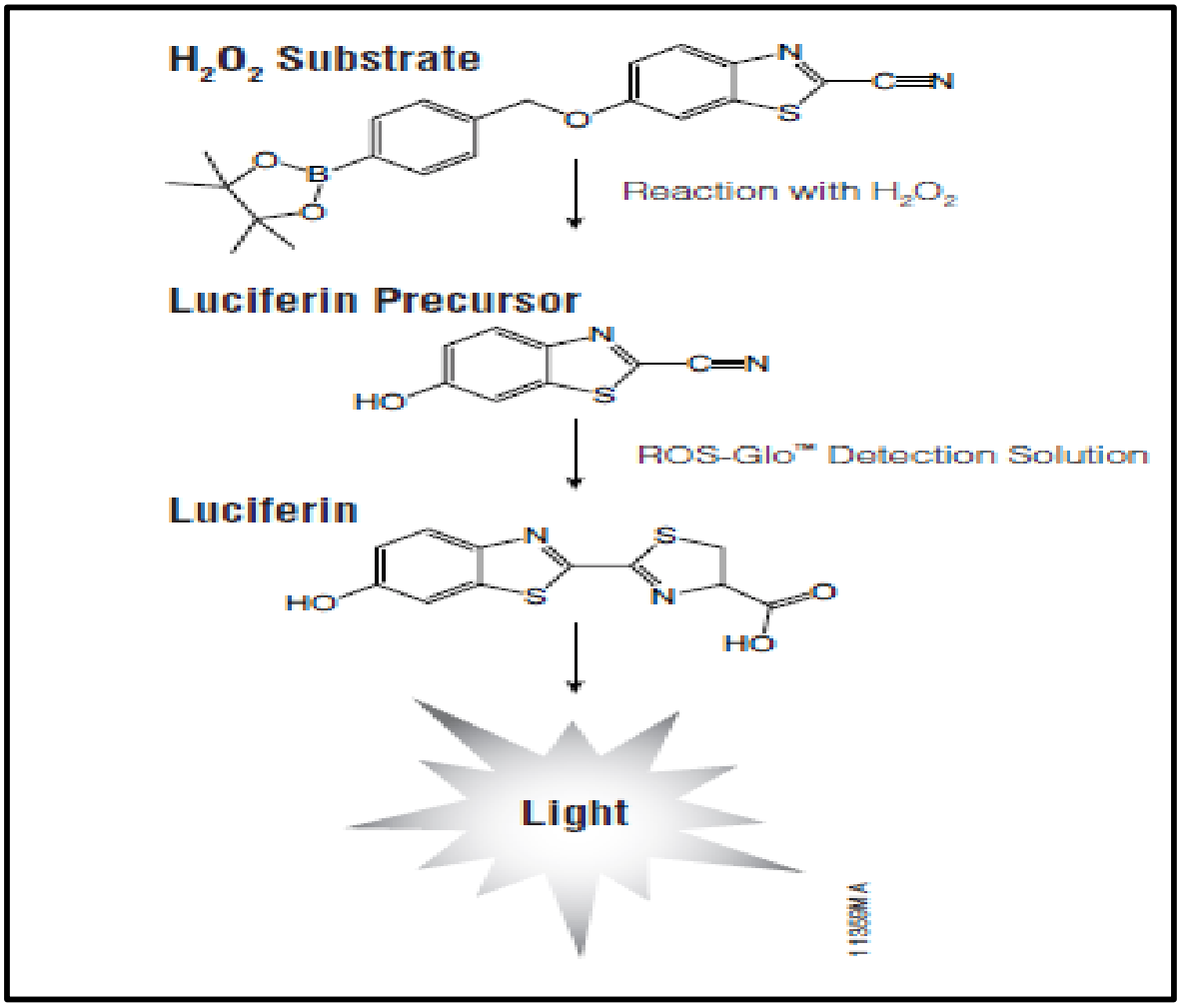

Figure 3.6 : The chemistry of ROS-Glo™ H_2O_2 Assay (Promega protocols).

3.5.5.2 Protocol

Hek293 cells were seeded into a 96-well plate with their respective treatments (80 µl) and allowed to attach in 24 h incubation (37 ^oC at 5 % CO_2). The H_2O_2 substrate was thawed and diluted accordingly. Thereafter, 20 µl of the H_2O_2 substrate was added into each well and incubated for 6 h (37 ^oC at 5 % CO_2). Subsequently, 100 µl of the ROS-Glo^{TM} detection solution was pipetted into each well and incubated for 20 min at RT. The luminescence was recorded using a Modulus™ microplate luminometer (Turner Bio-systems, Sunnyvale, USA) and was analysed as RLU.

3.5.6 Glutathione Assay

3.5.6.1 Principle

Glutathione is an antioxidant that can prevent damage to vital cellular components caused by ROS such as free radicals and lipid peroxides. This assay serves to quantify GSH levels based on the conversion of a luciferin derivative into luciferin in the presence of glutathione. This conversion is catalysed by glutathione *S*-transferase (GST). The signal generated is proportional to the amount of glutathione present in the sample (Figure 3.7).

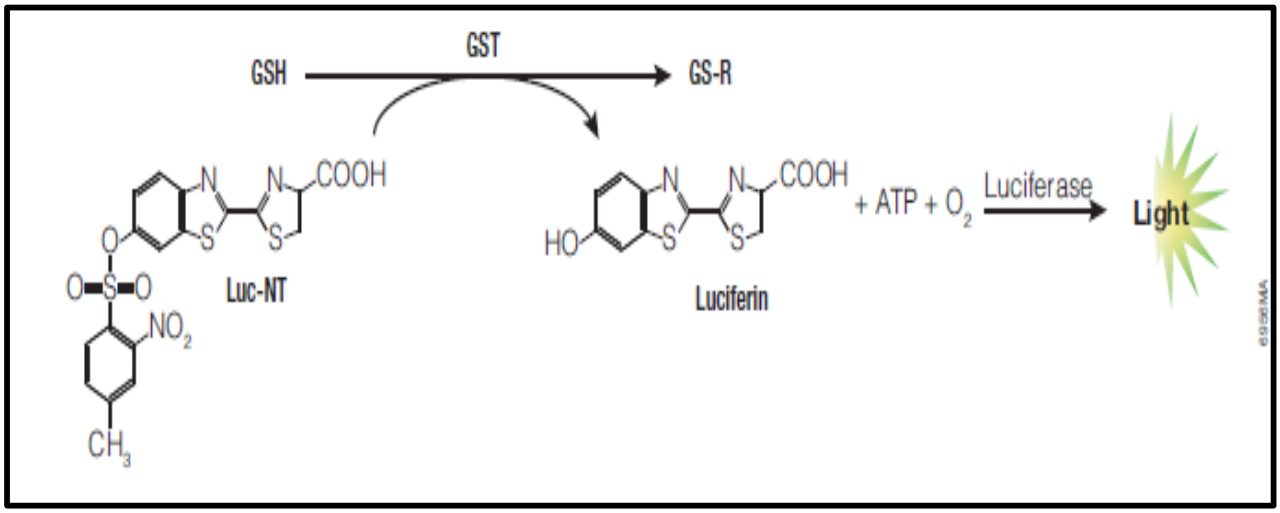

Figure 3.7 : GSH-Glo™ Glutathione assay overview (Promega protocols).

3.5.6.2 Protocol

In a 96-well white plate, 20,000 treated Hek293 cells were added and incubated (37 ºC at 5 % CO_2). GSH standards were prepared according to the manufacturers guidelines and added to the wells in duplicate. Thereafter 100 µl of the 2X GSH-Glo™ reagent was pipetted into each well. The plate was then incubated for 30 min at RT. Thereafter, 100 µl of the Luciferin Detection reagent was added into each well and briefly mixed before an incubation of 15 min at RT. The luminescence was then measured with the use of a Modulus™ microplate luminometer (Turner Bio-systems, Sunnyvale, USA) and recorded as RLU.

3.6 Single Cell Gel Electrophoresis (SGCE) Assay

3.6.1 Principle

DNA fragmentation in individual cells is detected by the comet assay (Figure 3.8). DNA fragmentation is a late characteristic of apoptosis, a result of the chain reaction that occurs due to the caspase cascade. Healthy, undamaged DNA maintains a highly organised, supercoiled structure within the nucleus whilst damaged DNA loses its structural organisation and migrates out of the nucleus when subjected to an electric field (Godard *et al*., 1999). When an electric field is applied to cells embedded in agarose gel, DNA migration out of the nucleus forms a 'comet', where the head contains intact, undamaged DNA and the tail contains damaged, fragmented DNA. The comet assay utilises fluorescence microscopy to visualise the presence and extent of DNA damage (Singh *et al*., 1988).

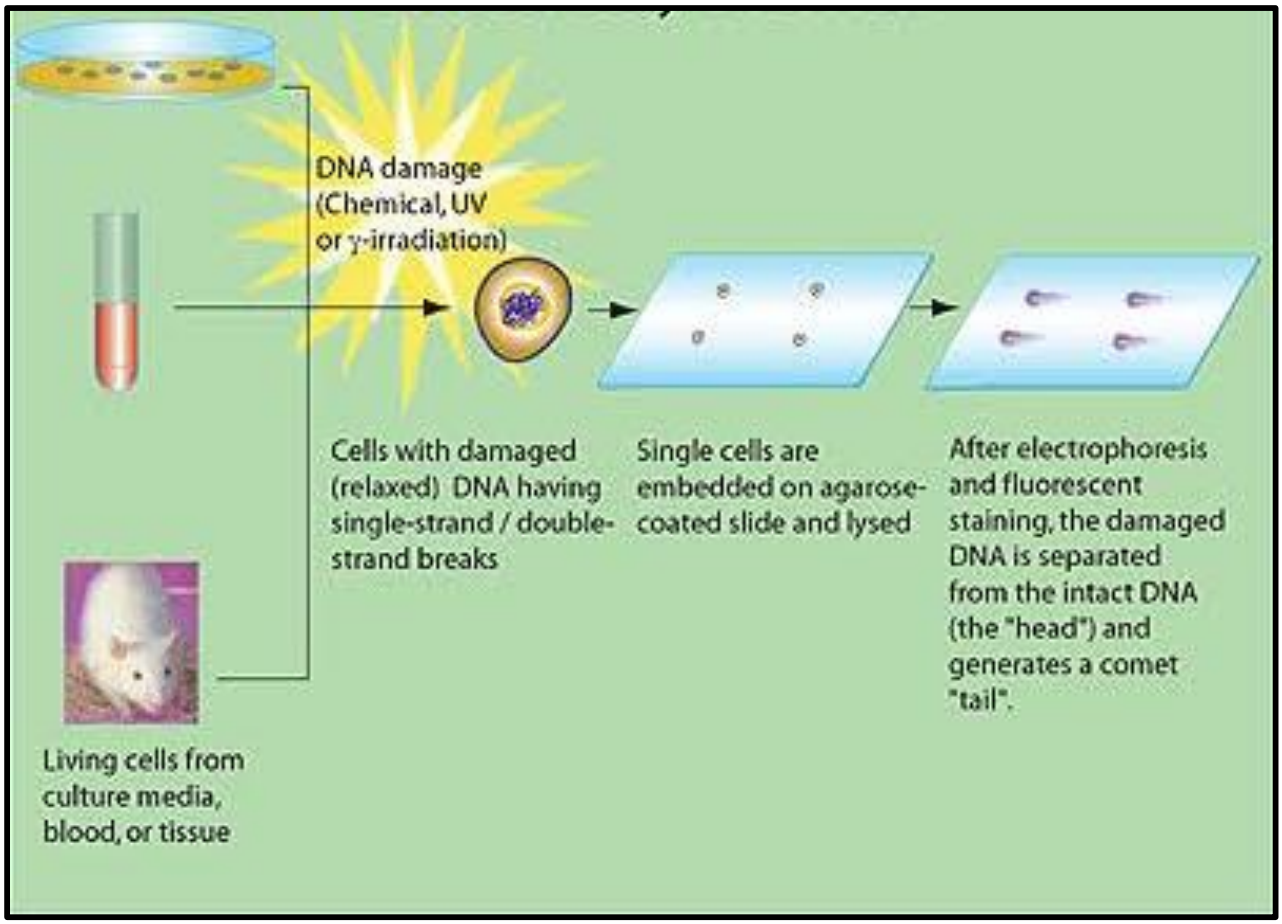

Figure 3.8 : An overview of the comet assay process (Sigma-aldrich protocol).

3.6.2 Protocol

Frosted end microscope slides were used for the SCGE assay (2 for each treatment). The slides were prepared with three layers: the first layer consisted of 2 % low melting point agarose (LMPA, 800 µl) covered with a coverslip at the top of the gel and was set at 4 ^{o}C for 10 min; the second layer consisted of 1 % LMPA (400 µl) with Gel Red (1 µl) and cell suspension (20,000 cells in 30 µl 0.1 M PBS) covered with a coverslip and solidified at 4 ^{o}C for 10 min; and the third and last layer consisted of 1 % LMPA (400 µl) covered with a coverslip at the top, which was left to set at 4 ^{o}C for 10 min. The same procedure was repeated for all the slides.

Coverslips were removed and solidified gels were submerged in cold cell lysis buffer [100 mM EDTA, 2.5 M NaCl, 1 % Triton X-100, 10 % DMSO, and 10 mM Tris (pH 10)] for 1 h at 4 °C. Thereafter, the slides were submerged in electrophoresis buffer [1 mM Na_2 EDTA (pH 13) and 300 mM NaOH] for 20 min at RT to allow for equilibration prior to electrophoresis (25 V, 35 min at room temperature) using a Bio-Rad compact power supply.

The slides were rinsed three times (5 min each) in (0.4 M Tris, pH 7.4) to neutralise the samples prior to replacement of coverslips. The slides were then viewed using a fluorescent microscope (Olympus IX51 inverted microscope, excitation: 510-560 nm; emission 590 nm). Images of 50 cells and comets were captured from each slide. The comet tail lengths were quantified using a Soft Imaging system and reported as tail lengths in µm.

3.7 Thiobarbituric acid reactive substances (TBARS) Assay

3.7.1 Principle

The detection of oxidative stress has relied largely on the quantification of compounds such as malondialdehyde (MDA), which are formed by degradation of initial products of free radical attack on membrane lipids (Oakes and Van Der Kraak, 2003). The reaction of MDA with 2-thiobarbituric

acid (TBA) produces a coloured product that can be detected at 532 nm (Figure 3.9). This assay is therefore one of the most widely used estimators of oxidative stress that measures MDA production, an indication of lipid peroxidation induced by oxidative stress.

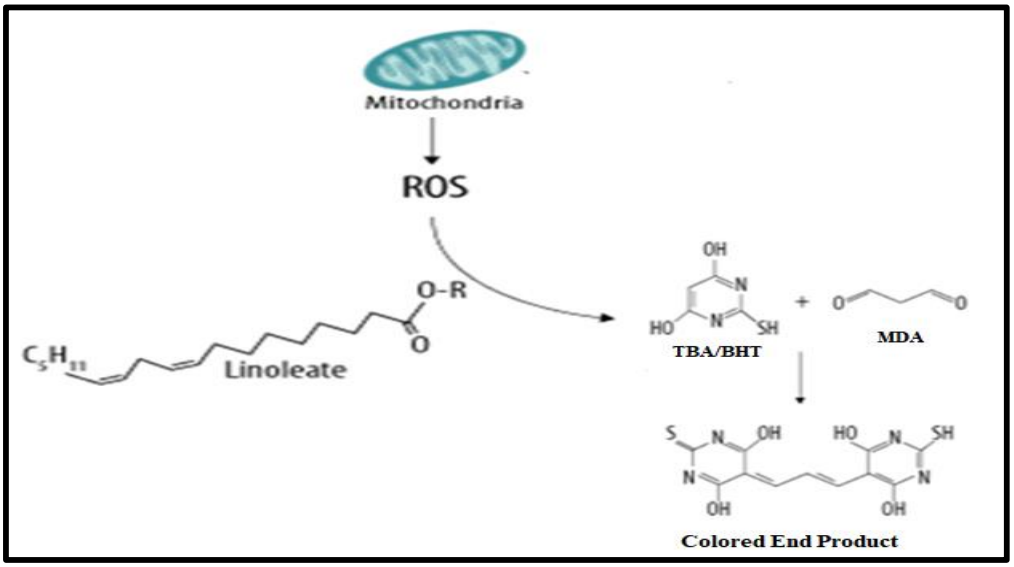

Figure 3.9 : Formation of MDA /TBA compound via the TBARS assay [Adapted from R&D systems protocol].

3.7.2 Protocol

The supernatants of each treatment (200 µl) were added into appropriately labelled, clean glass test tubes in duplicates containing 200 µl of 2 % phosphoric acid (H_2PO_4). A positive (containing MDA) and negative control (CCM only) was included in this experiment. Thereafter, 400 µl of TBA/Butylated hydroxytoluene (BHT) solution was added to every sample except the negative control, this tube received 400 µl of 3 mM HCl.

Each test tube was briefly vortexed, and the pH of each sample was adjusted to 1.5 using 1 M HCl. The tubes were subsequently boiled in a water bath for 15 min at 100 °C to allow for optimal hydrolysis of MDA-adducts. After the samples cooled to RT, 1500 µl of butanol was added to each tube to extract MDA by separating the solution into two phases. The tubes were then vortexed and allowed to stand for the distinction of the two phases.

Lastly 200 µl of the upper butanol phase in each test tube was transferred to a 96-well microtitre plate in duplicates. The absorbance was measured at 532 nm with a reference wavelength of 600 nm using a Bio-Tek µQuant spectrophotometer (USA).

3.8 Nitric Oxide Assay

3.8.1 Principle

Reactive nitrogen species (RNS) are formed when nitric oxide (NO) reacts with superoxide to produce peroxynitrite. It is therefore important to evaluate the production of NO to determine if nitrosative stress is present. The assay indirectly quantifies NO and therefore gives a measure of the RNS present.

The nitric oxide assay is a traditional method used to measure the conversion of L-[3H] arginine to L-[3H]citrulline. However, because nitric oxide is oxidised to nitrates and nitrites in biological samples, it is these end-products that are quantified in this two-step reaction assay used to measure oxidative stress. The Greiss reaction is used as follows: vanadium (III) chloride (VCl_3), sulphanilamide (SULF) and N-1-Naphthyl ethylenediamine dihydrochloride (NEDD) are each added in quick succession to facilitate reduction, inhibition of enzymatic reactions involving para-aminobenzoic acid and colour change (detected at 540 nm) respectively (Figure 3.10) (Beda and Nedospasov, 2005).

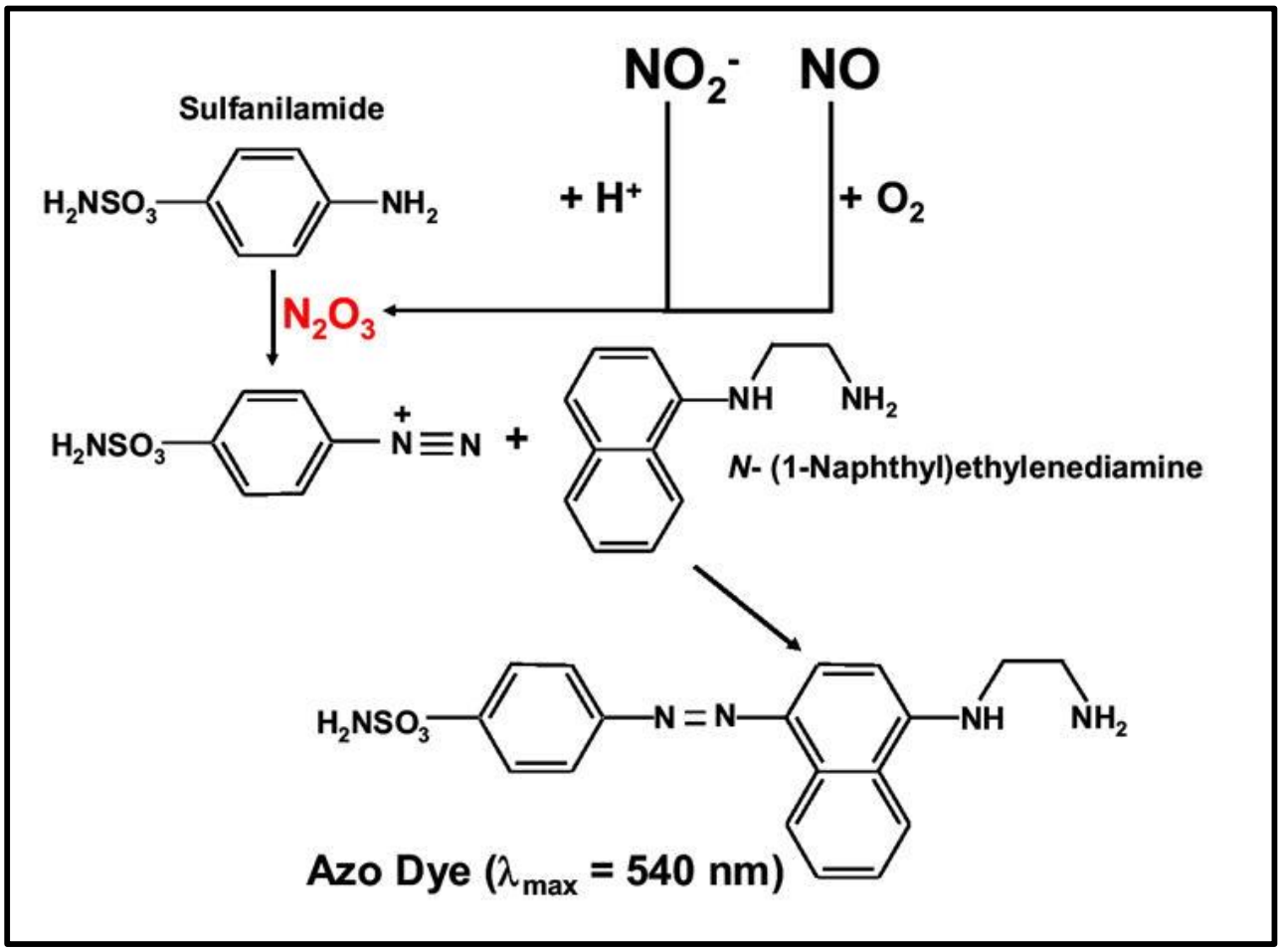

Figure 3.10 : Nitric oxide assay represented by a two-step azotisation reaction that produces a diazo product (Bryan and Grisham, 2007).

3.8.2 Protocol

Sodium nitrate standards were prepared with a concentration range of 0–200 µM and 50 µl of each standard as well as the respective treatments were plated into a 96 well plate in duplicate. Subsequently, 50 µl VCl_3 and 25 µl SULF were added in all the wells (standards and samples) followed by the addition of 50 µl NEDD. The plate was then incubated at 37 °C for 45 min. Following incubation, the plate was read and quantified using a Bio-Tek µQuant plate reader (USA) at a wavelength of 540 nm and a reference wavelength of 690 nm. A standard curve using the standards was then plotted and the concentration of RNS of the samples was extrapolated from the graph.

3.9 Western Blotting

3.9.1 Principle

Western blotting is an analytical technique used to detect the proteins in a homogenous sample. It relies on the principle that the proteins are separated through a sodium dodecyl sulfate (SDS)-Polyacrylamide gel using an electric field (Figure 3.11). The extent of migration is determined by the size of the proteins. The proteins are then transferred onto a nitrocellulose membrane and immunoprobing takes place for the actual western blot (Figure 3.12). Proteins are represented as bands at the site of the antigen-antibody reaction and the band width is proportional to the quantity of the respective protein (Mahmood and Yang, 2012). Antioxidant and apoptotic proteins were quantified via western blotting.

3.9.2 Protocol

Crude protein was isolated from treated cells using Cytobuster^{TM} reagent containing protease and phosphatase inhibitors (300 µl). Flasks were placed on ice for 15 min, and then cells were scraped off the flasks and transferred to 1.5 ml eppendorf tubes which were also placed on ice for a further 15 min. The cells were then centrifuged at 2 000 x g for 5 min (4 ^{o}C) to remove cellular debris. The crude protein obtained was quantified using the bichinchoninic acid (BCA) assay.

Bovine serum albumin (BSA) standards (0–1 mg/ml) were prepared to determine the concentration of the protein samples. The standards and samples were then pipetted (25 µl) in duplicate into a 96-well microtiter plate. The BCA reagent (198 µl BCA: 4 µl $CuSO_4$) was added in each well (200 µl) and incubated at 37 ^{o}C for 30 min. The absorbance was detected using Bio-Tek µQuant spectrophotometer (USA) at 562 nm. A standard curve was constructed and proteins were standardised to 1 mg/ml. Laemmli buffer (dH_2O, 0.5 M Tris-HCl (pH 6.8), glycerol, 10 % SDS, β-mercaptoethanol , 1 % bromophenol blue) was added to each sample (1:4, total volume 250 µl), and heated to 100 °C (5 min).

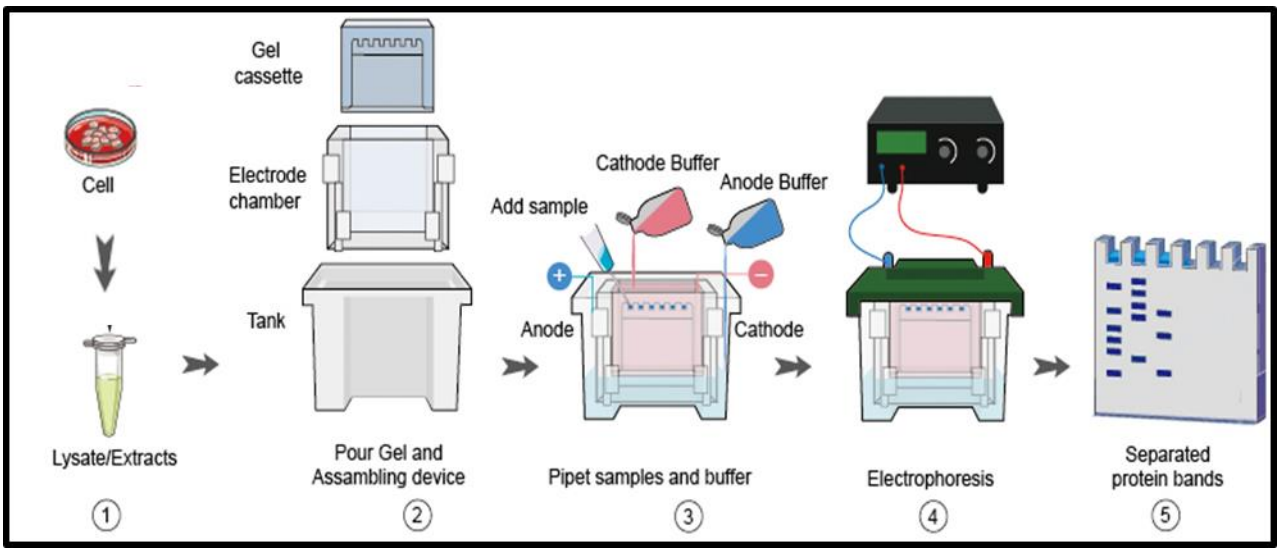

Figure 3.11 : Western blot procedure from sample preparation to protein electrophoresis [Adapted from Creative Diagnostics protocol].

The standardised, denatured proteins (25 µl) were loaded onto a SDS-polyacrylamide gel (10 % resolving gel and 4 % stacking gel) to separate proteins (1.5 h at 150 V) using running buffer (Tris, glycine, SDS, dH_20), after which transfer onto nitrocellulose membranes was achieved with transfer buffer (Tris, glycine, methanol, dH_2O) using the Transblot ®Turbo™ Transfer system (Bio-Rad). Membranes were blocked with 5 % BSA in Tween20 Tris-buffered saline (TTBS, 25 mM Tris (pH 7.5) 150 mM NaCl, 0.05 % Tween 20) for 2 h, and incubated with primary antibodies (GPx1 [#3286], SOD2 [#13141], Nrf2 [#12721], p53 [#48818], Bax [#5023], cPARP [#9542], catalase [#12980] and Hsp70 [#46477]) in 5 % BSA/TTBS (1:1000 dilution) overnight. The primary antibody was removed and membranes were washed five times with TTBS (10 min each), then incubated in secondary antibody (anti-rabbit IgG [#7074] or anti-mouse IgG [#70746]) as required, in 5 % BSA/TTBS (1:2500 dilution) for 2 h. Following incubation, membranes were washed with TTBS (5x 10 min each). Clarity Western ECL Substrate (Bio-Rad) (150 µl) was added to the membranes and images were captured using a Molecular Imager® Chemidoc™ XRS and BioRad imaging system and actin [#12141] as a loading control.

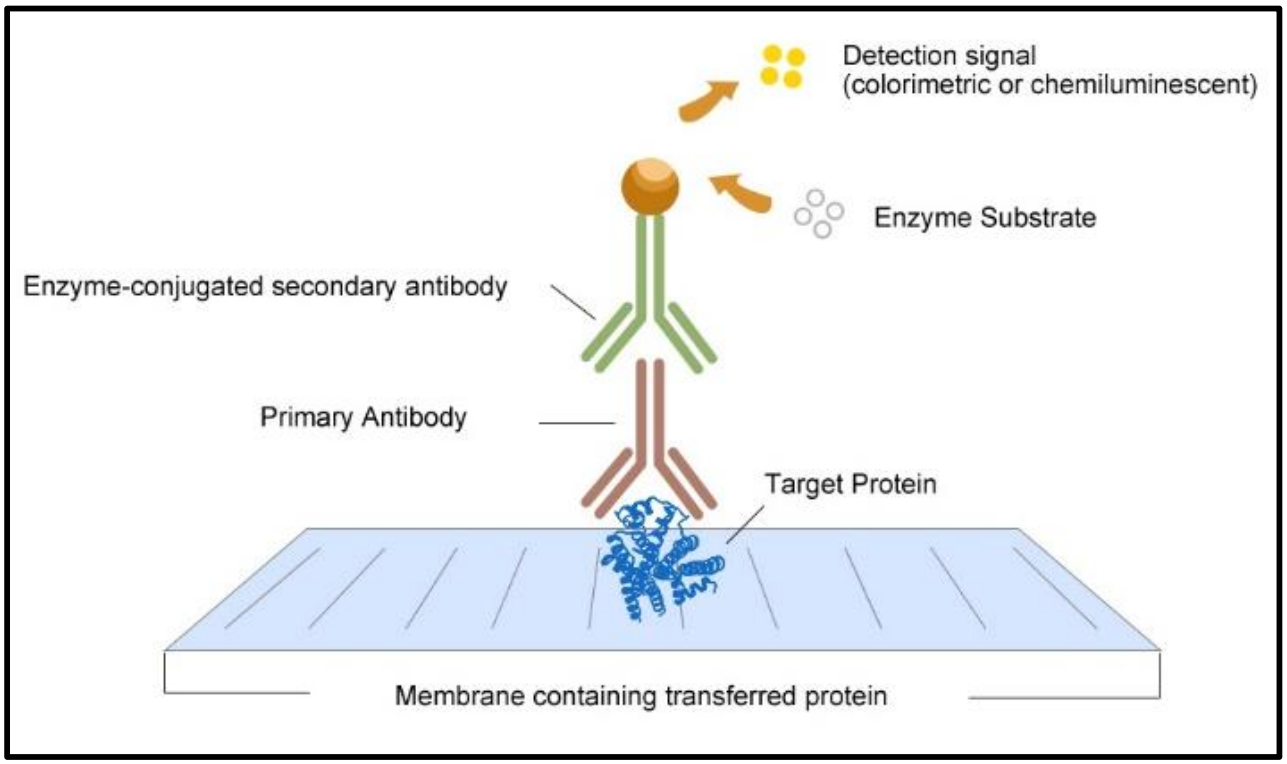

Figure 3.12 : Representation of immunoblotting illustrating the binding of a primary antibody onto the target protein, followed by the secondary antibody-enzyme conjugate. This then allows for the emission of a chemiluminescent detection signal (elabscience protocols).

3.10 Quantitative- Polymerase Chain Reactions (qPCR)

3.10.1 Principle

Quantitative- Polymerase Chain Reactions (qPCR) also known as real time PCR, is a reliable technique that both detects and measures products of the PCR process. When the PCR product is directly proportional to the amount of template DNA from the beginning of the PCR process, data is then collected in the exponential growth stage (Arya *et al*., 2005). The qPCR process occurs in two steps, first mRNA is isolated from cells, and then the mRNA is reverse transcribed to single-stranded complementary DNA (cDNA). Furthermore, qPCR is characterised by the addition of a fluorescent dye, SYBR green to the master mix (SYBR green, nuclease-free water, forward and reverse primer) (Hernandez-Rodriguez and Ramirez, 2012).

3.10.2 Protocol

Cells with the relevant treatments were washed once with 0.1 M PBS. The total RNA was isolated in a series of steps. Briefly, 500 µl PBS and 500 µl Triazol was added to the flask and incubated at RT for 5 min. Thereafter, the flasks were scraped and the contents were transferred to 1.5 ml micro-centrifuge tubes and stored at -80 ºC overnight. Thereafter, 100 µl chloroform was added to the thawed samples and mixed vigorously for 15 sec. The samples were incubated at room temperature for 3 min. The micro-centrifuge tubes were then centrifuged (12000 x g, 4 ˚C for 15 min), and the upper aqueous layer was transferred to a new 1.5 ml micro-centrifuge tube, which was placed on ice. Subsequently, 250 µl isopropanol was added to each sample and incubated on ice for 2 h before being returned to -80 ºC overnight. Samples were thawed again and centrifuged (12000 x g, 4 ºC for 20 min). The resulting pellet contained the total RNA and was washed with 500 µl cold 75 % ethanol. Samples were then centrifuged again (7400 x g, 4 ºC for 15 min). All ethanol was discarded and the pellet was left to air-dry, before re-suspending in 15 µl RNase-free water. RNA samples were incubated at RT (3 min). A Thermo Scientific™ Nanodrop 2000 (Thermo Fisher Scientific; Johannesburg, South Africa) machine was used to determine the quality and quantity of the isolated RNA. The absorbance ratio of 260 nm/280 nm was used to determine purity of samples (~2). RNA samples were standardised to a concentration of 1000 ng/µl with RNase-free water and stored at -80 °C until required.

RNA was reverse transcribed to cDNA as per manufacturers' guidelines using the iScript™ cDNA Synthesis kit (Bio-Rad; 107-8890): a 20 µl reaction volume containing 1 µl iScript™ reverse transcriptase, 4 µl 5X iScript™ reaction mix and the RNA template (2000 ng) made up in nuclease free water. Thermocycler conditions were set to 25 °C for 5 min, 42 °C for 30 min, 85 °C for 5 min and a final hold at 4 °C. The cDNA was diluted 1:4 to obtain a final volume of 100 µl.

Gene expression was analysed using the iQ™ SYBR Green Supermix (Bio-Rad; 170-880), according to the manufacturer's instructions. Briefly, 1.5 µl cDNA template, 1 µl sense primer, 1 µl antisense primer, 5x iScript reaction mix and nuclease free water was made up to a reaction volume of 25 µl. The gene of interest was SOD2 [forward 5'-CAGCCCAGCCTGCGTAGACGG-3'; reverse 5'-GCGTTGATGTGAGGTTCCAG-3' (57 °C)]. All primers were obtained from Inqaba Biotechnologies (Pretoria, South Africa).

The qPCR experiments were conducted using the CFX Touch™ Real Time PCR Detection System (Bio-Rad; Hercules, California, United States). The assay was run with three replicates per treatment. GAPDH [forward 5'-CGTGGAAGGACTCATGACCA-3'; reverse 5' -GCCATCACGCCACAGTTTC-3' (57 °C)] was used as a housekeeping gene and was amplified simultaneously under the same conditions as the treatment samples. The reaction was subjected to an initial denaturation (95 °C, 4 min), followed by 37 denaturation cycles (95 °C, 15 sec), an annealing phase (57 °C, 40 sec), and an extension phase (72 °C, 30 sec).

The acquired data was analysed using the method described by Livak and Schmittgen (2001) represented as fold-change in mRNA expression ($2^{-\Delta\Delta CT}$) relative to the control (Livak and Schmittgen, 2001).

3.11 Statistical analysis

The data acquired was expressed as mean optical density with standard deviations for the MTT assay and IC_{50} was determined using the dose-response inhibition equation (Log inhibition versus variable slope). For the data obtained from subsequent assays, the One-way ANOVA and an unpaired t-test with Welch's correction was performed. The data was represented as means ± standard deviations. A *p* value of 0.05 was considered to be statistically significant. These statistical tests are available on GraphPad prism version 5.0 software.

CHAPTER 4: RESULTS

The results obtained from the experiments elaborated in Chapter 3 will be outlined. Each reported result is accompanied by a graphical illustration that shows the major changes that occurred following treatment with FB_1, allicin and a combination of FB_1 and allicin.

4.1 Methyl-thiazol-tetrazolium (MTT) Assay

The dose-response of FB_1 and allicin was assessed using the MTT assay and generated the IC_{50} for use in this study. The cell viability decreased to 76 % at 50 µM FB_1, 72 % at 125 µM FB_1 and 29 % at 250 µM FB_1; yielding an IC_{50} of 215 µM FB_1 (Figure 4.1A). Allicin induced a decrease in cell viability to consistently less than 30 % from 5 – 150 µM, and an IC_{50} of 3.905 µM was derived (Figure 4.1B).

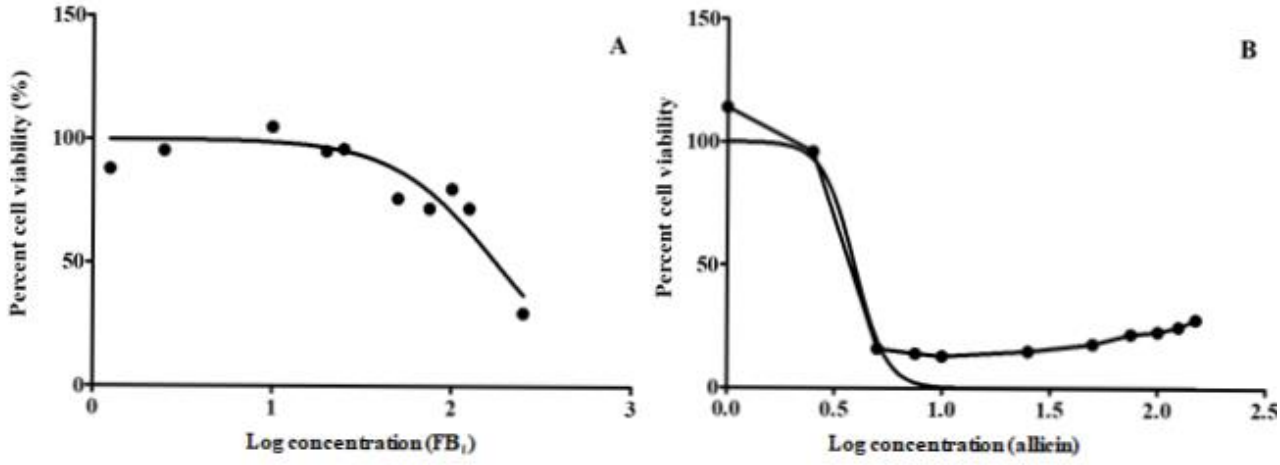

Figure 4.1 : The percent cell viability of Hek293 cells treated with varying concentrations of FB_1 (A) and allicin (B) respectively was decreased with increasing doses when compared to an untreated control. The curves were used to calculate the IC_{50} of both exposures.

4.2 CytoTox-ONE™ Homogeneous Membrane Integrity Assay

The CytoTox-ONE™ homogeneous membrane integrity assay was used to measure the release of LDH from cells as an indicator for cytotoxicity (Figure 4.2). Basal LDH level in untreated cells was 16700 ± 0.002983 RLU. Individual FB_1 and allicin treated Hek293 cells showed a slight reduction in

cell membrane damage, whilst LDH release in combined FB_1+allicin treated cells increased to 35150 ± 6450 RLU, indicating significant cell membrane damage and cytotoxicity.

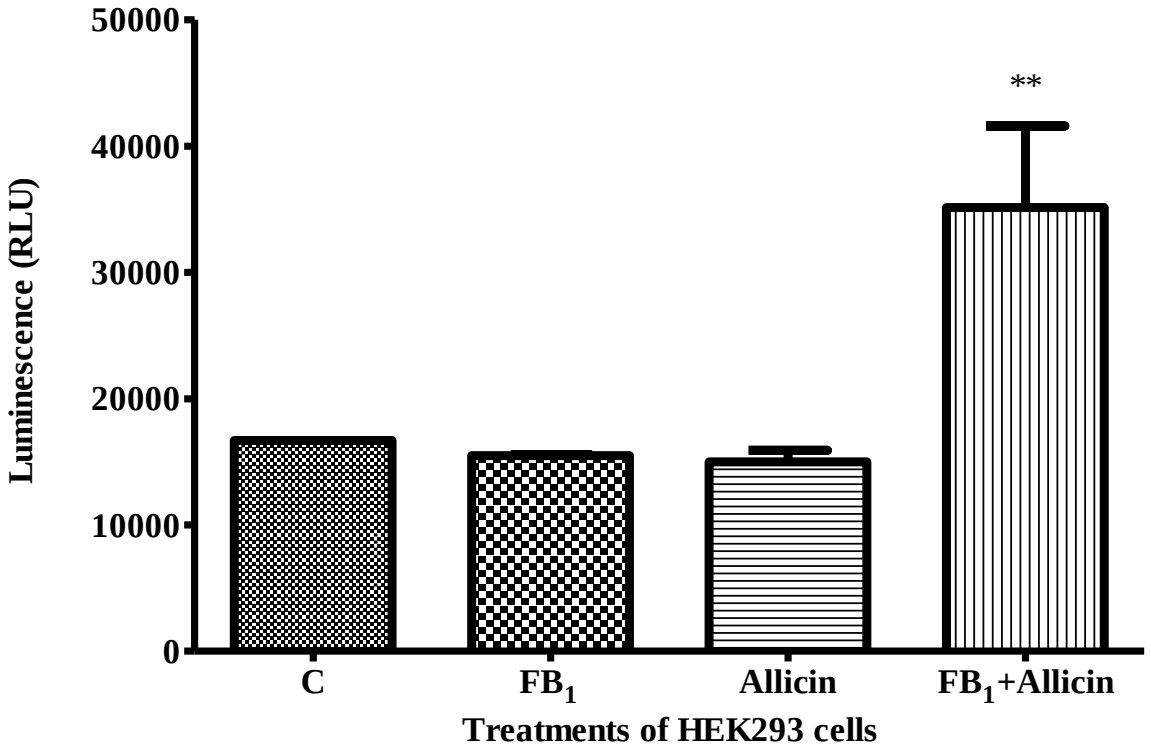

Figure 4.2: Slightly decreased LDH levels in individual FB_1 and allicin treated cells. LDH was significantly increased to 35150 ± 6450 RLU in combined FB_1+allicin treated cells. One-way ANOVA with Tukeys post-test – $p = 0.0015$.

4.3 Mitochondrial ToxGlo™ Assay

The mitochondrial integrity was assessed by measuring protease activity (Figure 4.3). There was a decrease in the mitochondrial integrity of FB_1 treated cells, while a 1.65-fold increase occurred in allicin treated cells and combined FB_1+allicin treatment restored mitochondrial integrity to control levels (313.0 ± 100.6).

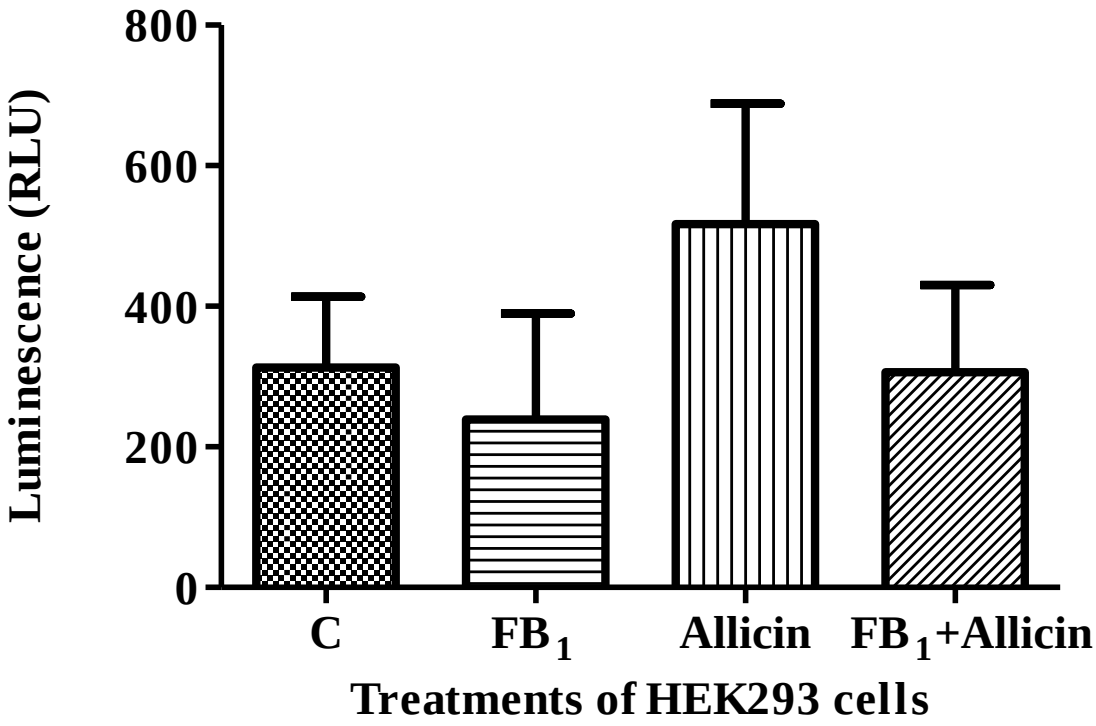

Figure 4.3 : Decrease in mitochondrial integrity of FB_1 treated cells ($p = 0.7102$), an increase in allicin treated cells ($p = 0.3797$) and a slight decrease in FB_1+allicin treated cells compared to the control.

4.4 Adenosine Triphosphate (ATP) Assay

The ATP concentration in Hek293 cells was assessed using luminometry. There was a significant increase in ATP levels for all treatments (Figure 4.4). FB_1 exposure resulted in a 50 % increase in ATP concentration ($p = 0.0003$). Allicin caused a slightly greater increase of 1.62-fold ($p = 0.0024$), while a significant 1.69-fold increase was observed in the combined FB_1+allicin treatment ($p < 0.0001$) when compared to the control (8989000 ± 76750).

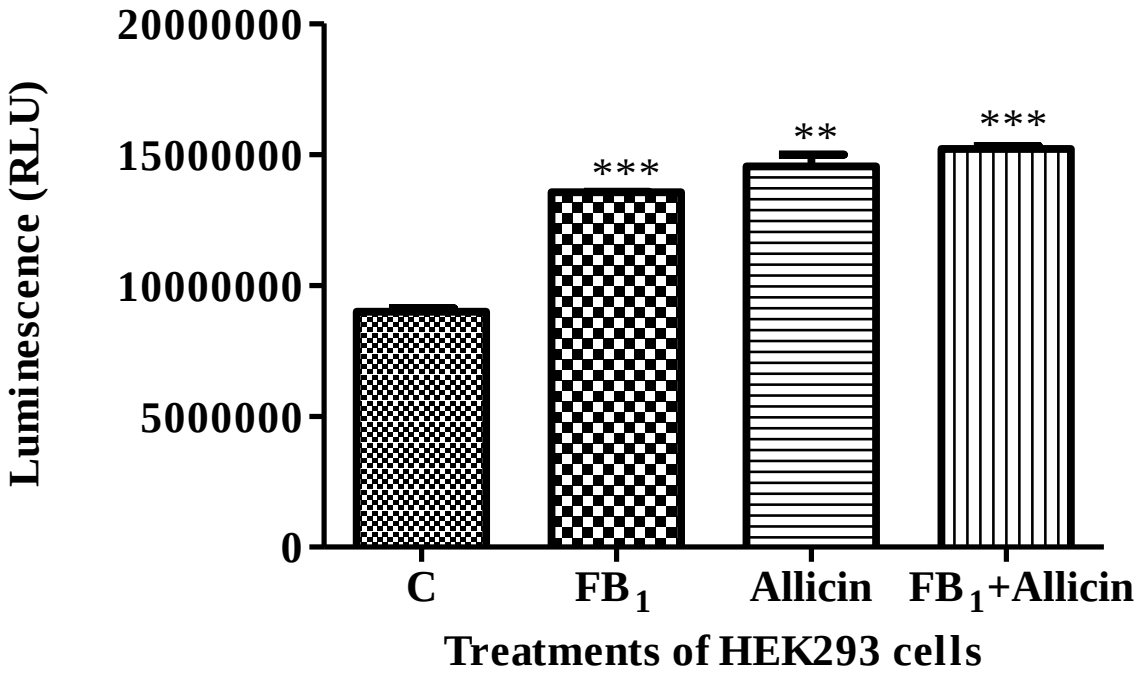

Figure 4.4: Significantly increased ATP levels in all HEK293 cell treatments relative to the control (8989000 ± 76750).

4.5 Free radicals

4.5.1 Reactive oxygen species

This assay measures the amount of H_2O_2 in the cell. The results demonstrate increased levels of H_2O_2 in all treatments (Figure 4.5A) with a 1.43-fold (p = 0.0671) in FB_1, 1.06-fold in allicin (p = 0.5369) and 1.66-fold in FB_1+allicin (p = 0.0002) treated cells compared to the control (63430 ± 4343).

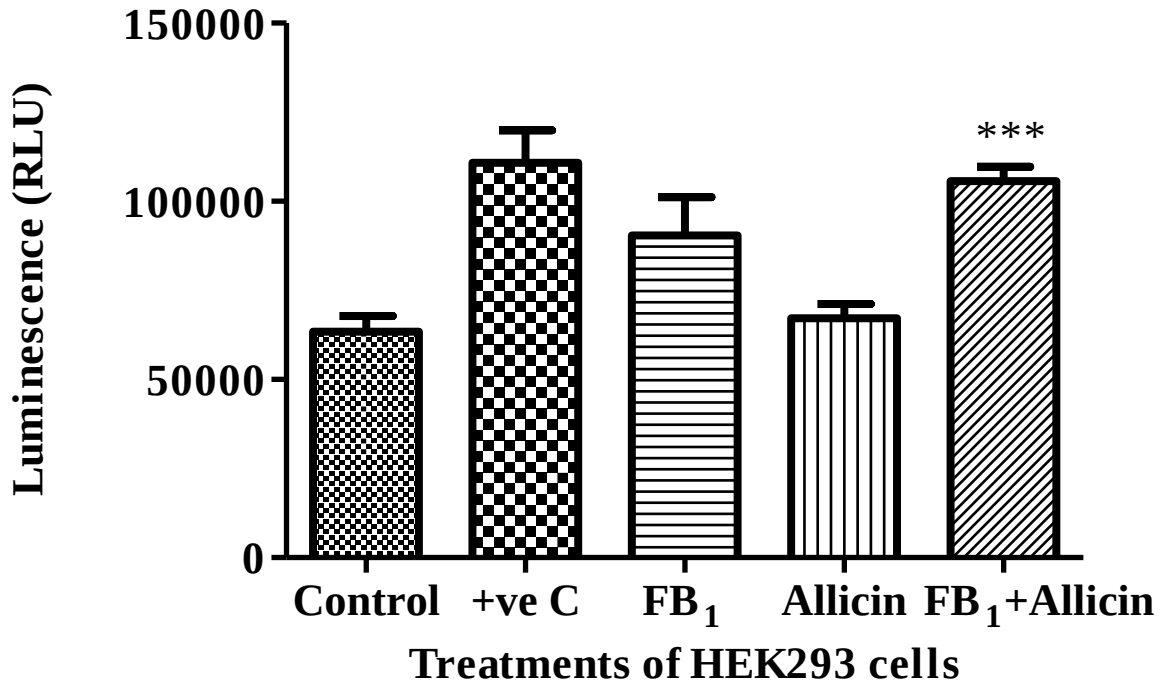

Figure 4.5A : Increased H_2O_2 levels in all HEK293 cell treatments relative to the control (63430 ± 4343).

4.5.2 Nitric Oxide Assay (NOS)

This assay measures the production of RNS. All three treatments showed a slight decrease in RNS formation (Figure 4.5B). Treatment with FB_1 causing a 33 % decrease in RNS (p = 0.0177), while allicin and FB_1+allicin resulted in 1.24-fold and 1.49-fold decreases respectively relative to control (11.14 ± 0.7021).

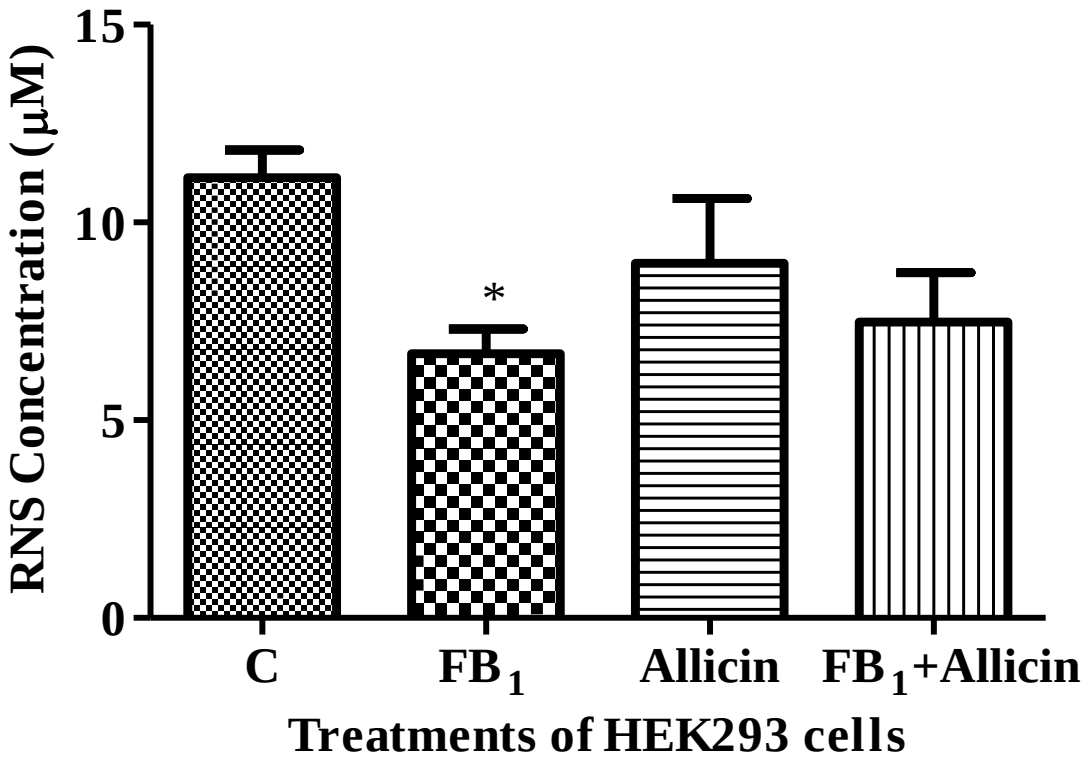

Figure 4.5B : Decreased levels of RNS formation in all three HEK293 cell treatments relative to the control (11.14 ± 0.7021).

4.6 Thiobarbituric Acid Reactive Substances (TBARS) Assay

ROS-induced lipid peroxidation as an oxidative stress marker was assessed by quantifying extracellular levels of MDA. Extracellular MDA levels were significantly reduced for all treatments of Hek293 cells (Figure 4.6). A 1.92-fold decrease in FB_1 ($p < 0.0001$), 2.28-fold decrease in allicin ($p < 0.0001$) and a 1.27-fold decrease in combined FB_1 + allicin ($p = 0.0001$) treated cells was noted compared to the control (0.5855 ± 0.009887).

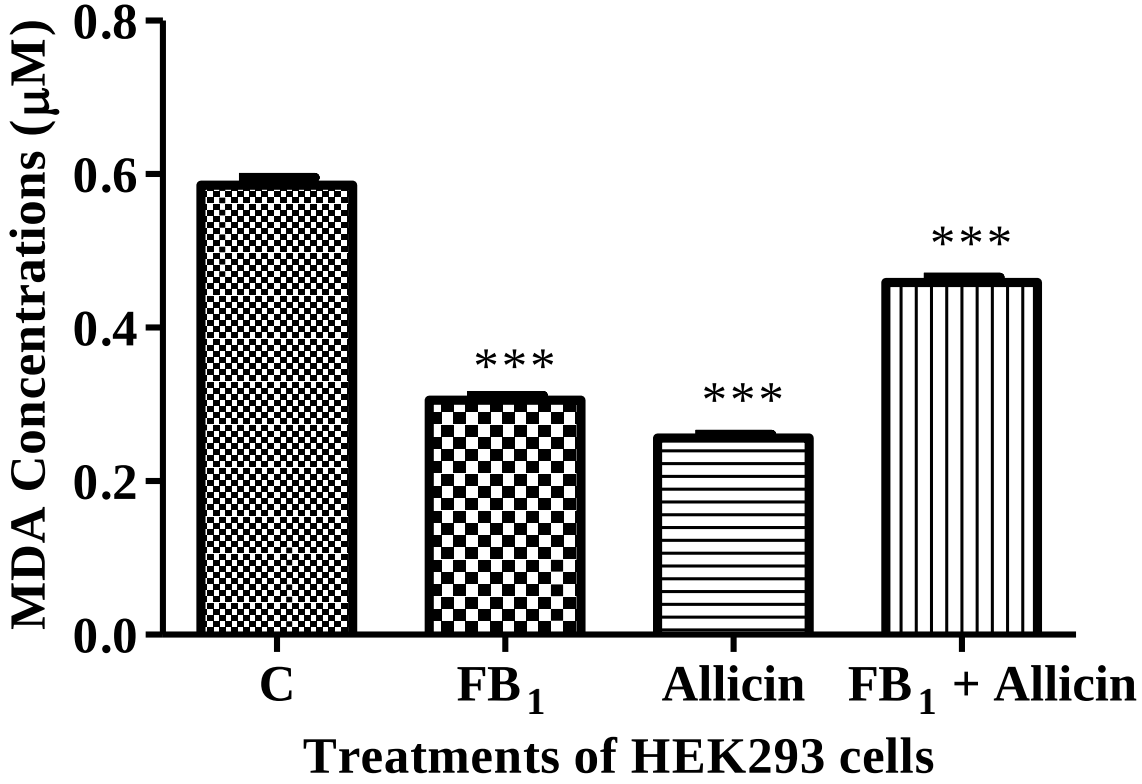

Figure 4.6 : Significantly reduced levels of extracellular MDA in all HEK293 treatments relative the control (0.5855 ± 0.009887) - *** significantly different from the control.

4.7 Glutathione (GSH) Assay

The GSH concentration was measured as a marker for intracellular antioxidant capacity. The results showed that FB_1 did not significantly alter GSH concentration (Figure 4.7). However, a 1.34-fold decrease and 1.66-fold decrease in the allicin (p = 0.0017) and combined FB_1+allicin (p = 0.0025) treated cells was noted compared to the control (1.225 ± 0.02307) (Figure 4.7).

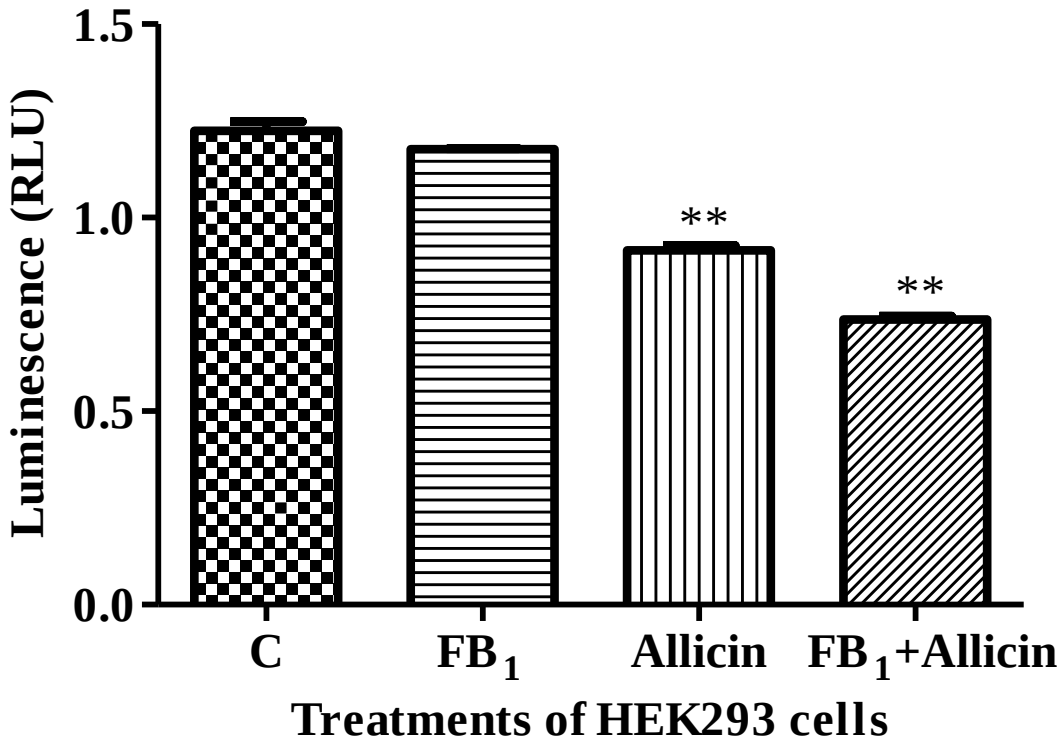

Figure 4.7: GSH concentrations relative to the control (1.225 ± 0.02307) show slight decrease in FB_1 treatment and significant decrease in both allicin (p = 0.0017) and combined FB_1+allicin (p = 0.0025) treated HEK293 cells.

4.8 Single Cell Gel Electrophoresis (SCGE) Assay

The comet assay was used to measure the length of comet tails as an indicator of DNA damage. All HEK293 cell treatments increased DNA damage shown by the significant increase in comet tail length (Figure 4.8). FB_1 increased by 1.5-fold (p < 0.0001), allicin increased by 1.29-fold and FB_1+allicin increased by 1.47-fold compared to the control (8.634 ± 0.4910).

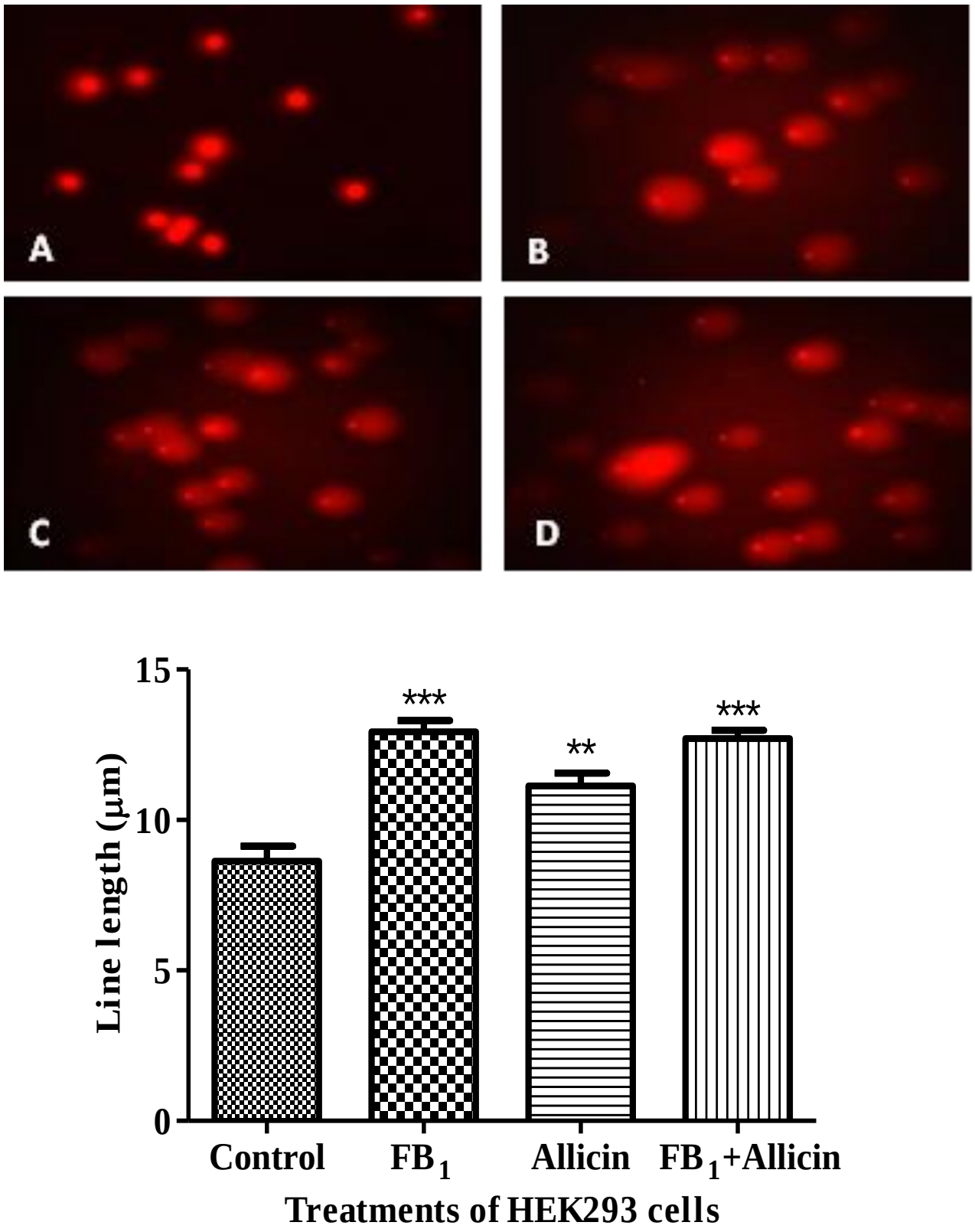

Figure 4.8 : Control cells (A) displayed an intact core of DNA, while FB_1 (B), allicin (C) and combined treatment (D) all caused migration of fragmented DNA from the nucleus, forming a comet tail. Significantly increased comet tail lengths were visualised for all HEK293 treatments relative to the control (8.634 ± 0.4910).

4.9 Caspases

The activity of caspases 8, 9 and 3/7 were assessed using luminometry. Caspases 8 (Figure 4.9A) and 9 (Figure 4.9B) demonstrate a significant upregulation in all Hek293 cell treatments: caspase 8 increased by 1.68-fold in FB_1 ($p = 0.0003$), 1.94-fold in allicin ($p = 0.0008$) and 2.33 in FB_1+allicin ($p = 0.0023$) treated cells relative to the control (2204000 ± 10750), and caspase 9 increased by 1.53-fold in FB_1 ($p < 0.0001$), 1.85-fold in allicin ($p < 0.0001$) and 2.24-fold in FB_1+allicin treated cells ($p < 0.0001$) relative to the control (5112000 ± 56180). Caspase 3/7 activity (Figure 4.9C) was significantly increased by 2.19-fold in the allicin-treated cells ($p < 0.0001$) and doubled in the combined treatment FB_1 + allicin treatments ($p < 0.0001$) when compared to the control (261700 ± 2835).

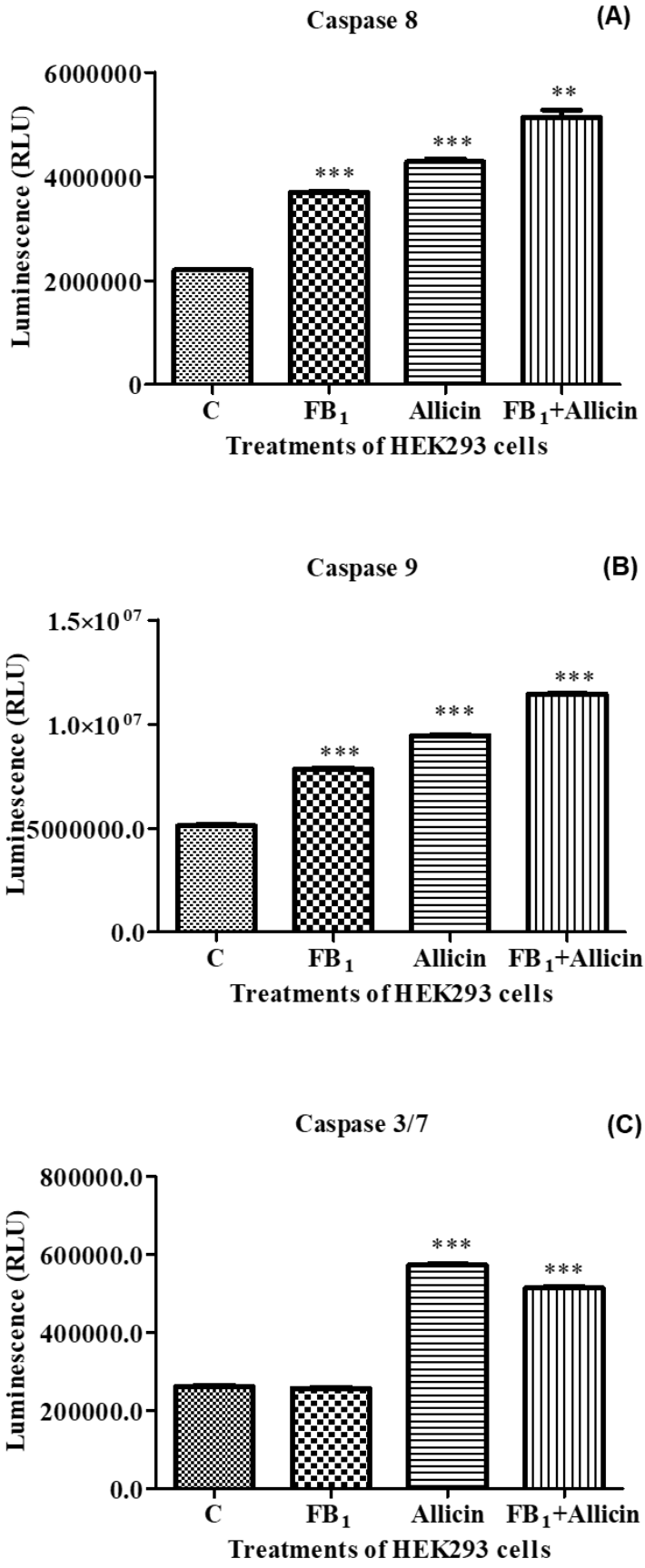

Figure 4.9: Caspase activity following cell exposure to FB_1, allicin and FB_1+allicin. (C) Executioner caspase 3/7 showed a slight decrease in FB_1 treated cells and a significant increase in subsequent treatments (****p < 0.0001*). (B) Initiator caspase 8 (A) and 9 were significantly upregulated for all treatments.

4.10 Western blots

Western blotting was used to determine oxidative stress (Figure 4.10A) and apoptotic protein (Figure 4.10B) expression.

Oxidative stress markers included SOD2, catalase, GPx1, Nrf2 and HSP70 (Figure 4.10A). SOD2 was significantly downregulated for all Hek293 cell treatments presenting with a 1.42-fold decrease in FB_1, a 1.72-fold decrease in allicin and a 2.75-fold decrease in FB_1+allicin relative to the control (2.208 ± 0.03848). Likewise, catalase expression was decreased for all treatments, and the most significant depletion was noted in the combined treatment. In contrast, all three treatments significantly upregulated the expression of GPx1 relative to the control, with the upregulation less significant in the combined treatment. The expression of Nrf2 was also upregulated with a synergistic effect in the FB_1+allicin compared to the control (0.3734 ± 0.1084). HSP70 expression was not markedly deviated from the control, with only slight increases occurring in the FB_1 and combined treatments.

Apoptotic markers probed for were Bax, cPARP and p53 (Figure 4.10B). Bax was significantly increased relative to the control. Allicin increased Bax expression slightly more that FB_1 alone. However, allicin treatment did not result in PARP cleavage, as was noted in the FB_1 and FB_1+allicin treatments. p53 was increased by 1.22-fold for FB_1, but the allicin increase was not significant and the combined FB_1+allicin treatment was unchanged when compared to the control.

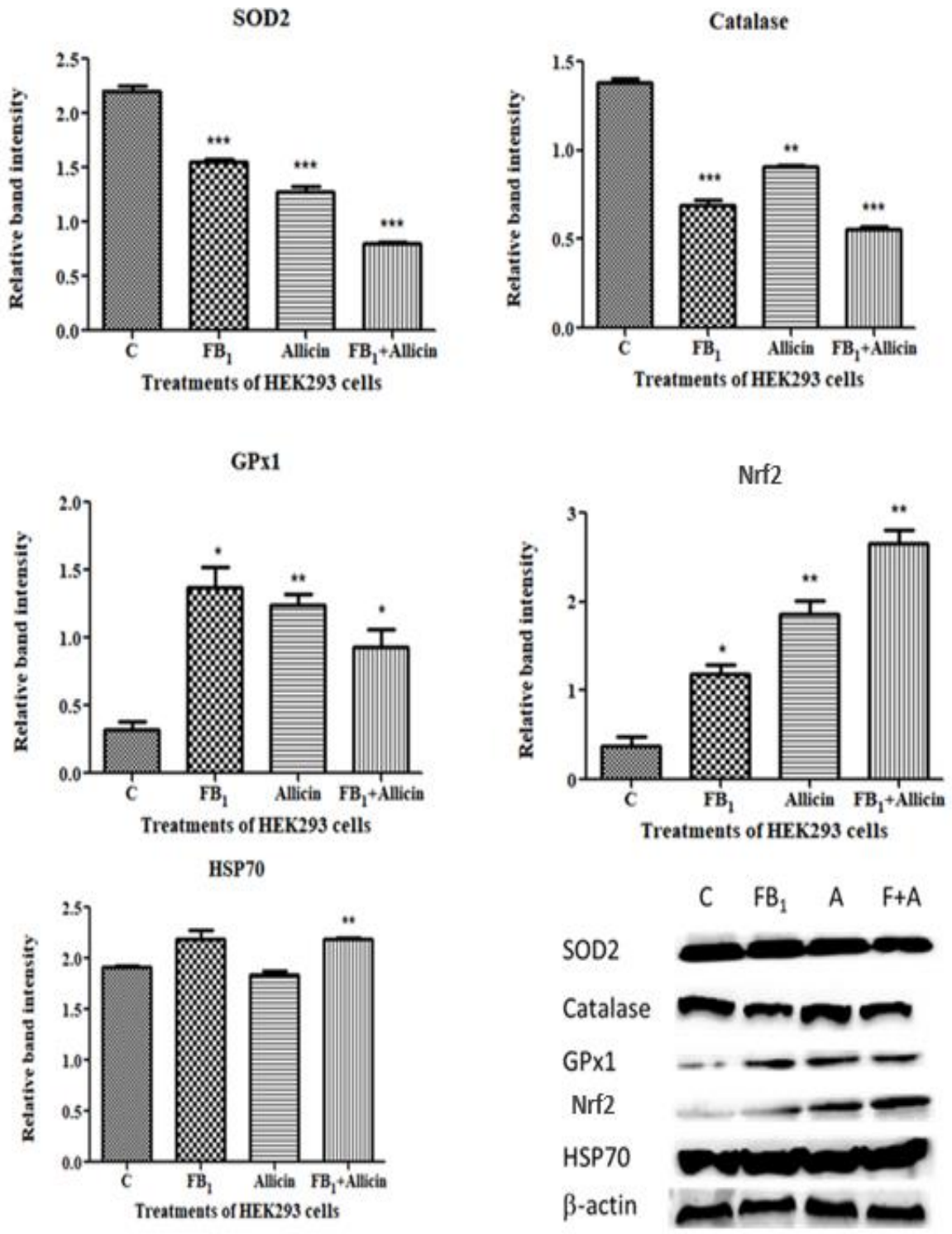

Figure 4.10A: Protein expression for oxidative stress following HEK293 treatments. Nrf2 was upregulated for all treatments relative to the control (0.3734 ± 0.1084). HSP70 was only decreased in the allicin treatment. The expression of GPx1 was upregulated in all treatments. SOD2 expression was significantly downregulated. Catalase was overall decreased for all treatments.

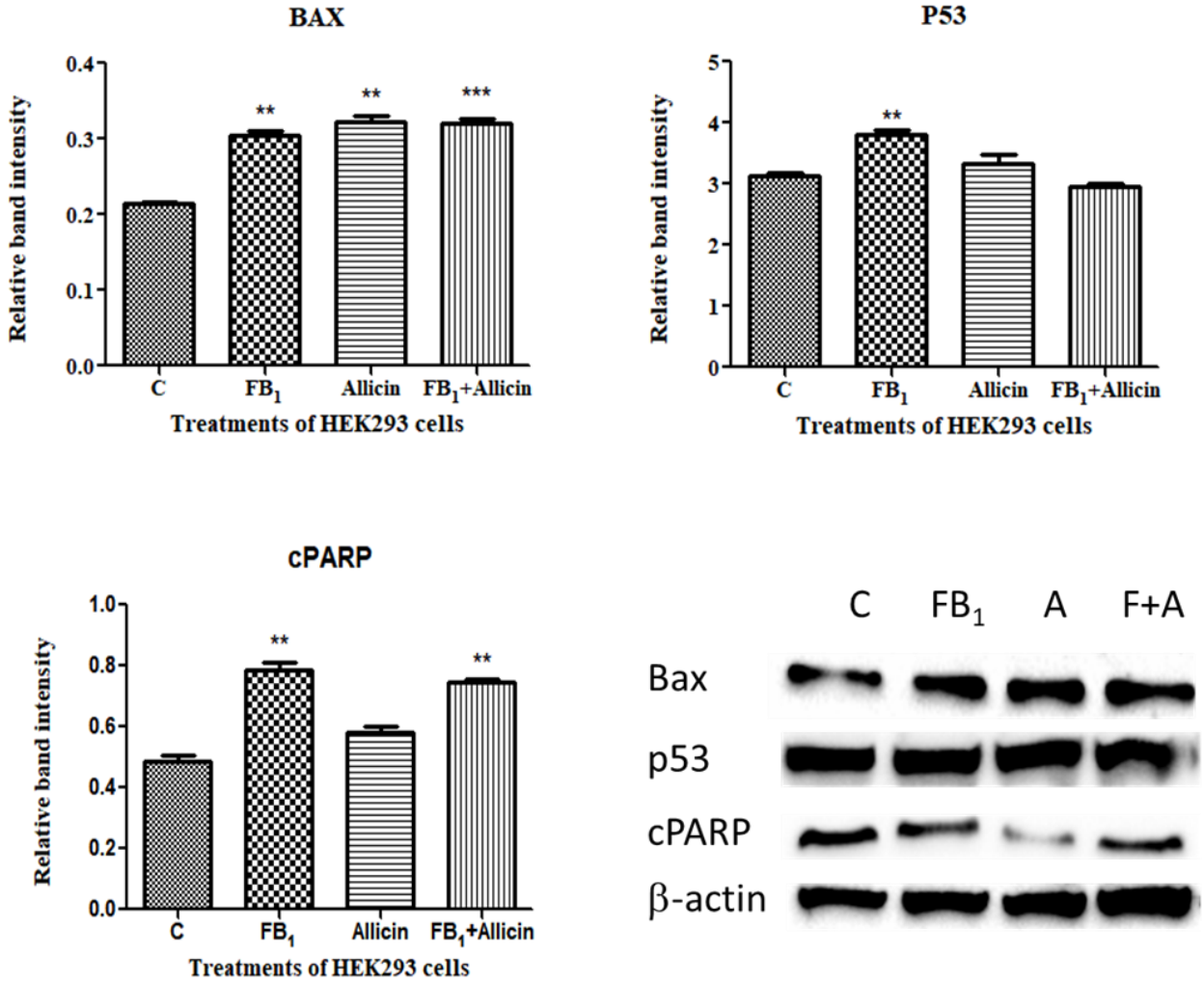

Figure 4.10B: Protein expression for apoptotic markers following Hek293 cell treatments. BAX was significantly increased for all treatments. p53 was upregulated for both FB_1 and allicin at 1.22-fold and 1.06-fold respectively. cPARP expression was increased for all treatments relative to the control (0.4867 ± 0.02153).

4.11 Quantitative- Polymerase Chain Reactions (qPCR)

Hek293 treatments were assessed to determine the mRNA levels of SOD2 (Figure 4.11). FB_1 and allicin increased mRNA levels. The combined FB_1+allicin treatment decreased the mRNA levels of SOD2 relative to the control (0.9725 ± 0.02496).

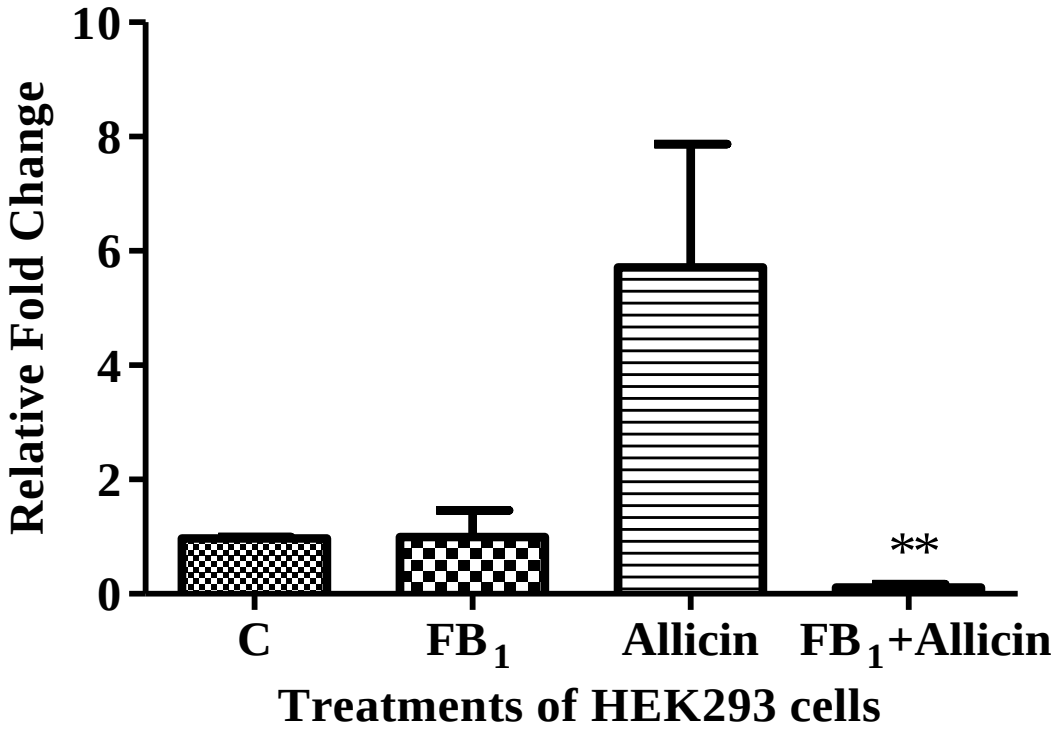

Figure 4.11: SOD2 was increased for both FB_1 and allicin at 1.02-fold and 5.87-fold respectively. The combined FB_1+allicin treatment was significantly decreased.

CHAPTER 5: DISCUSSION

FB_1 is a vastly studied mycotoxin produced as a secondary metabolite of *Fusarium verticillioides* known to contaminate crops. Studies have shown FB_1 to be toxic in multiple cell lines of human and animal origin (Berek *et al*., 2001, Schmale and Munkvold, 2009). Although its mechanism of action remains unclear, many investigations performed on animal models demonstrate its effects on sphingolipid metabolism (Riley *et al*., 1994) and more recently, a new epigenetic influence (Chuturgoon *et al*., 2014) has been suggested . Overall, these mechanisms may result in dysregulation of protein synthesis and a variety of cytotoxic effects that include oxidative stress and cell death. The ubiquitous mycotoxin, FB_1, is geographically associated with OC in humans and liver/kidney cancer in rats (Voss *et al*., 1993, Howard *et* al., 2001, Khan *et al*., 2018b). A recent study investigated its effects in HepG2 liver cancer cells (Chuturgoon *et al*., 2014). However, its role in kidney toxicity in humans has not been investigated.

Garlic, a common medicinal plant has been used to treat various ailments over centuries. Its biological component allicin has been found to be responsible for many health benefits including anti-cancer properties through inhibition of cellular proliferation, inducing apoptosis and antioxidant activity to alleviate oxidative stress (Mikaili *et al*., 2013, Gruhlke *et al*., 2016). This study therefore sought to investigate the toxic effects of FB_1 in Hek293 cells. In addition, the ability of allicin to ameliorate their effects was studied.

Cytotoxicity was investigated using the MTT assay, which yielded an IC_{50} of 215 µM and 3.905 µM for FB_1 and allicin respectively (Figure 4.1 A and B). The IC_{50} in other studies varied for different cell lines, eliciting effects at different concentrations (Agarwal, 1996, Ha and Yuan, 2004, Liao *et al*., 2009, Suddek, 2014) The decreased cell viability indicates that both FB_1 and allicin negatively influenced the mitochondrial ability to oxidise the MTT salt to its formazan product. Various studies

have shown that at varying concentrations, FB_1 decreases viability (Rumora *et al*., 2002, Chuturgoon *et al*., 2015). However, Myburg *et al*. (2002) showed that FB_1 had limited cytotoxicity in human OC SNO cells over 24 h and 48 h respectively (Myburg *et al*., 2002). With regards to allicin, studies have shown that it inhibits cell proliferation. According to Prager-Khoutorsky *et al*. (2007) this may be due to its effects on tubulin, thus the mitotic spindle will not form and cell division will be inhibited (Prager-Khoutorsky *et al*., 2007, Gruhlke *et al*., 2016).

Mitochondrial function is pivotal both in the production of ATP and activation of the intrinsic pathway of apoptosis. In addition, mitochondria also produce ROS as by-products of energy metabolism. Thus, determination of mitochondrial health is important. In this study, only allicin demonstrated increased mitochondrial integrity relative to the control (Figure 4.3). Furthermore, ATP production was increased by all treatments (Figure 4.4). The increased ATP implies an active electron transport chain. Where mitochondrial integrity is compromised, that will inevitably result in the production of ROS. Allicin increased mitochondrial integrity. When ATP production is increased in intact mitochondria, there would be less leakage of electrons and therefore less iROS formed (Brookes et al., 2004), as demonstrated by the results. iROS were increased by FB_1 and only slightly increased for allicin, while allicin failed to prevent iROS production in the presence of FB_1 (Figure 4.5A); in both instances, mitochondrial integrity was slightly lower relative to the control. However, RNS were decreased for all treatments (Figure 4.5B). Oxidative stress results from the production of ROS and an inadequate antioxidant response. In this study, the presence of oxidative stress is suggested by increased HSP70 in all treatments, where it appears that allicin potentiates the effects of FB_1, as well as Nrf2 which was synergistically increased in the combined treatment (Figure 4.10A).

An antioxidant response includes mobilisation of SOD2, catalase, GPx1, GSH and Nrf2. While downregulation of SOD2 protein expression occurred in all treatments (Figure 4.10A) its gene expression particularly increased (Figure 4.11) in the allicin treatments. Therefore, superoxide

conversion to H_2O_2 could not take place using SOD2. However, it may have been converted intracellularly by SOD1, a cytosolic enzyme isoform of SOD, into H_2O_2 (Birben *et al*., 2012). Khan *et al*. (2018b) demonstrated a decreased expression of SOD2 at 0-20 µM FB_1 doses in SNO cells (Khan *et al*., 2018a). In addition, underlying pathways including protein degradation play a major role in mRNA gene expression and protein concentration. This is supported by Scholze *et al.* (2011) whose study found an increase in the gene expression of SOD1 in chronic kidney disease patients coupled with decreased protein expression (Scholze *et al*., 2011, Krueger *et al*., 2016). Catalase, the antioxidant responsible for the conversion of H_2O_2 to H_2O was also decreased in the FB_1 and in the combined treatment.

The increased iROS levels therefore were not associated with SOD2 or catalase. The principle intracellular antioxidant is GSH; its depletion is usually an indication of oxidative stress (Forman *et al*., 2009). GSH was decreased by allicin and in the combined treatment (Figure 4.7), this is not surprising since allicin is a thiol agent that is known to oxidise GSH to GSSG, this has been confirmed by Gruhlke *et al.* (2016) who showed a decrease in GSH following administration of allicin (Gruhlke *et al*., 2016). In addition, GPx1 was increased (Figure 4.10A), which may account for the depletion of GSH; when GPx1 is activated to convert H_2O_2 to H_2O, GSH is oxidised to GSSG. The reduction of GSSG requires glutathione reductase (GR) and NADPH, a cofactor derived from the pentose phosphate pathway (Patra and Hay, 2014).

In the presence of cellular stress, HSP70 is expressed as a primary response sensor following protein misfolding (El Golli-Bennour and Bacha, 2011). This makes HSP70 a biomarker for oxidative stress. In this study, HSP70 indicated the presence of oxidative stress in the FB_1 and combined treatment (Figure 4.5A). While an increase in ROS production (H_2O_2) is noted in the FB_1 and combined treatment (Figure 4.5A), the antioxidant response is mobilised to ameliorate this effect. This is indicated by a depletion in the cellular antioxidants such as GSH, SOD and catalase (Figure 4.7, 10A).

Increased levels ROS are known to inactivate or deplete antioxidant enzymes (Lushchak, 2015), resulting in an accumulation or inadequate removal of ROS and oxidative stress (Fukai and Ushio-Fukai, 2011). For the allicin treatment, this utilisation of antioxidants kept H_2O_2 within normal limits, and oxidative stress was not present as indicated by HSP70 protein expression (Figure 4.10A). Increased Nrf2 (Figure 10A) explains the upregulation in the expression of GPx1 which in turn used up GSH to detoxify H_2O_2 (Ma, 2013), and is supported by research which shows that allicin elevates the levels of Nrf2 for the expression of other antioxidants to alleviate oxidative stress (Bat-Chen et al., 2010). A study on HepG2 cells demonstrated that transcription of antioxidant proteins was regulated by Nrf2 in FB_1-treated cells (García-Trejo *et al*., 2016, Arumugam *et al*., 2018). However, the Nrf2 response that results in increased SOD gene expression in allicin-treated cells, does not occur in the combined treatments (Figure 4.11). Therefore, despite the enhanced protein expression of Nrf2 following combination treatment, an accompanying replenishment of SOD will not occur. Thus allicin will not ameliorate the effects of FB_1. Given the reduced SOD gene expression relative to the FB_1-treatment suggests that allicin may increase oxidative stress in FB_1-treated cells.

While iROS were increased, there was no corresponding increase in lipid peroxidation (Figure 4.6). This decrease triggers the upregulation of antioxidant response molecules to maintain cellular homeostasis (Ayala *et al*., 2014). However, there was increased DNA fragmentation (Figure 4.8), which may be mediated by oxidative stress. When there is DNA damage, p53 is activated to initiate repair, cause cell cycle arrest or apoptosis. p53 was only slightly increased by FB_1 and allicin (Figure 4.10B) and was decreased in the combined treatments therefore repair mechanisms were not activated by allicin. DNA fragmentation is a morphological feature of apoptosis; therefore, in this study it may represent a late-stage marker for apoptosis.

Apoptosis is a programmed cell death mechanism facilitated by a family of proteins called caspases; in this study caspase activities were evaluated. In all treatments, the initiator caspases 8 and 9 were

upregulated (Figure 4.9A, B) which suggests that apoptosis is initiated via the extrinsic and intrinsic pathways; indeed, both FB_1 and allicin have been shown to induce apoptosis (Dragan *et al*., 2001, Oommen *et al*., 2004, Minervini *et al*., 2004, Bat-Chen *et al*., 2010) Upon activation, these caspases initiate the apoptotic cascade that culminates in the cleavage of caspase 3/7 known as the executioner of apoptosis. However, the results show that FB_1 did not increase caspase 3/7 (Figure 4.9C). It is possible that inhibitors of apoptosis (IAPs) may have blocked caspase 3/7 activation, by blocking apoptosis downstream of cytochrome c release by binding to and inhibiting active caspase 9 within the apoptosome, preventing downstream activation of procaspase 3/7. Chuturgoon *et al*.(2015) showed that BIRC 8, an IAP, was increased following FB_1 administration in HepG2 cells, which may have been responsible for lack of execution caspase 3/7 activity despite caspase 9 activation (Chuturgoon *et al*., 2015). In addition the presence of mitochondrial proteins Smac/DIABLO and Omi/HtrA2 antagonise this inhibitory action (Burke *et al*., 2010, Parrish *et al*., 2013). Furthermore, HSP70 is an anti-apoptotic protein that can inhibit apoptosis upstream of caspase 3/7 activation; this can therefore be supported by the observed increase in HSP70 in FB_1 treated cells (Figure 4.10A). A study on animal models also showed that FB_1 increased the expression of HSP70 and this is inclined with our findings (Kócsó *et al*., 2018).

An overall increase in caspase levels was noted in allicin and combined allicin and FB_1-treated Hek293 cells (Figure 4.9C) suggesting caspase-dependant activation of apoptosis. These findings are in agreement with a study done by Oommen *et al*. (2004) on human cervical and colon cancer cells wherein allicin halted cancer growth through induction of caspase-dependent apoptosis. Their results showed an increase in 3, 8 and 9 as well as PARP cleavage (Oommen *et al*., 2004). Bax is responsible for the formation of mitochondrial pores to release cytochrome c. Our results demonstrated an overall increase in Bax expression (Figure 4.10B). Alternatively, mitochondrial toxicity associated with allicin treatment could be responsible for cytochrome c release and caspase activation.

Activated caspase 3/7 results in the cleavage of iCAD and PARP forming CAD and cPARP respectively. CAD is a DNase that cleaves DNA into 180 bases per unit and is associated with the fragmentation of DNA as seen in Figure 4.9. The PARP are a family of proteins that assist in DNA damage and repair by binding to and repairing detected single and double-stranded DNA breaks. Caspase 3 cleaves PARP and therefore renders it inactive. Oommen *et al*. (2004) showed increased cPARP in human cervical and human colon cancer cells (Oommen *et al*., 2004). Likewise, 10 µM FB_1 treatment of SNO cells also caused an increase in cPARP (Khan *et al*., 2018a). Thus, allicin increased induction of apoptosis in the presence of FB_1, which was expected since oxidative stress was present. If increased apoptosis is accompanied by compensatory cell proliferation to replenish damaged cells, then cancer could result. This is of particular concern since the combined treatment also decreased DNA repair.

CHAPTER 6: CONCLUSION

This study sought to explore mechanisms of toxicity exerted by FB_1 in a human kidney cell line coupled with the potential therapeutic properties of allicin on FB_1 treated Hek293 cells. The results show that FB_1 and allicin cause a decrease in cell viability. All three treatments increased MDA in conjunction with increased ATP production. However, H_2O_2 concentration was not altered by allicin. The activation of an antioxidant response occurred; Nrf2 and GPx1 were upregulated but SOD2 and catalase were decreased, suggesting alternative modes of oxidant detoxification. Apoptosis was triggered in all treatments via both intrinsic and extrinsic pathways, but execution in the FB_1 treatment was not caspase-dependent. Cumulatively, FB_1 and allicin individually trigger apoptosis, but only FB_1 induced oxidative stress. When combined, a possible synergistic relationship is demonstrated in the expression of proteins. In addition, allicin caused decreased SOD2 gene expression in the presence of FB_1 despite increased Nrf2 upregulation. Therefore, allicin did not exert a therapeutic effect on FB_1-treated Hek293 cells.

Following findings from this study, further investigations on the effects of IAP in FB_1-induced apoptosis is recommended. The inflammatory pathway as a consequence of both allicin and FB_1 on *in vitro* and *in vivo* models is also of interest for future studies.

While more research is required, allicin should not be recommended as a supplement to ameliorate the cytotoxic effects of FB_1. This study only tested the IC_{50} concentrations of FB_1 and allicin. Perhaps expanding the range of treatment concentrations can give a better picture of the interaction between FB_1 and allicin.

REFERENCES

ABADO-BECOGNEE, K., MOBIO, T. A., ENNAMANY, R., FLEURAT-LESSARD, F., SHIER, W., BADRIA, F. & CREPPY, E. E. 1998. Cytotoxicity of fumonisin B1: implication of lipid peroxidation and inhibition of protein and DNA syntheses. *Archives of toxicology,* 72**,** 233-236.

ABATE, G., MSHANA, R. & MIÖRNER, H. 1998. Evaluation of a colorimetric assay based on 3-(4, 5-dimethylthiazol-2-yl)-2, 5-diphenyl tetrazolium bromide (MTT) for rapid detection of rifampicin resistance in Mycobacterium tuberculosis. *The International Journal of Tuberculosis and Lung Disease,* 2**,** 1011-1016.

ABBES, S., BEN SALAH-ABBÈS, J., JEBALI, R., YOUNES, R. B. & OUESLATI, R. 2016. Interaction of aflatoxin B1 and fumonisin B1 in mice causes immunotoxicity and oxidative stress: Possible protective role using lactic acid bacteria. *Journal of immunotoxicology,* 13**,** 46-54.

ABUJA, P. M. & ALBERTINI, R. 2001. Methods for monitoring oxidative stress, lipid peroxidation and oxidation resistance of lipoproteins. *Clinica chimica acta,* 306**,** 1-17.

AGARWAL, K. C. 1996. Therapeutic actions of garlic constituents. *Medicinal research reviews,* 16**,** 111-124.

AMAGASE, H. 2006. Clarifying the real bioactive constituents of garlic. *The Journal of nutrition,* 136**,** 716S-725S.

ARUMUGAM, T., PILLAY, Y., GHAZI, T., NAGIAH, S., ABDUL, N. S. & CHUTURGOON, A. A. 2018. Fumonisin B 1-induced oxidative stress triggers Nrf2-mediated antioxidant response in human hepatocellular carcinoma (HepG2) cells. *Mycotoxin research***,** 1-11.

ARYA, M., SHERGILL, I. S., WILLIAMSON, M., GOMMERSALL, L., ARYA, N. & PATEL, H. R. 2005. Basic principles of real-time quantitative PCR. *Expert review of molecular diagnostics,* 5**,** 209-219.

AYALA, A., MUÑOZ, M. F. & ARGÜELLES, S. 2014. Lipid peroxidation: production, metabolism, and signaling mechanisms of malondialdehyde and 4-hydroxy-2-nonenal. *Oxidative medicine and cellular longevity,* 2014.

BACCARELLI, A. & BOLLATI, V. 2009. Epigenetics and environmental chemicals. *Current opinion in pediatrics,* 21**,** 243.

BAIG, S., SEEVASANT, I., MOHAMAD, J., MUKHEEM, A., HURI, H. & KAMARUL, T. 2017. Potential of apoptotic pathway-targeted cancer therapeutic research: Where do we stand? *Cell death & disease,* 7**,** e2058.

BAT-CHEN, W., GOLAN, T., PERI, I., LUDMER, Z. & SCHWARTZ, B. 2010. Allicin purified from fresh garlic cloves induces apoptosis in colon cancer cells via Nrf2. *Nutrition and cancer,* 62**,** 947-957.

BEDA, N. & NEDOSPASOV, A. 2005. A spectrophotometric assay for nitrate in an excess of nitrite. *Nitric Oxide,* 13**,** 93-97.

BEREK, L., PETRI, I. B., MESTERHAZY, A., TÉREN, J. & MOLNÁR, J. 2001. Effects of mycotoxins on human immune functions in vitro. *Toxicology in vitro,* 15**,** 25-30.

BHANDARI, P. R. 2012. Garlic (Allium sativum L.): A review of potential therapeutic applications. *International Journal of Green Pharmacy (IJGP),* 6.

BIRBEN, E., SAHINER, U. M., SACKESEN, C., ERZURUM, S. & KALAYCI, O. 2012. Oxidative stress and antioxidant defense. *World Allergy Organization Journal,* 5**,** 9.

BRENNER, C. & KROEMER, G. 2000. Mitochondria--the death signal integrators. *Science,* 289**,** 1150-1151.

BROOKES, P. S., YOON, Y., ROBOTHAM, J. L., ANDERS, M. & SHEU, S.-S. 2004. Calcium, ATP, and ROS: a mitochondrial love-hate triangle. *American Journal of Physiology-Cell Physiology,* 287**,** C817-C833.

BRUNELLE, J. K. & ZHANG, B. 2010. Apoptosis assays for quantifying the bioactivity of anticancer drug products. *Drug Resistance Updates,* 13**,** 172-179.

BRYAN, N. S. & GRISHAM, M. B. 2007. Methods to detect nitric oxide and its metabolites in biological samples. *Free Radical Biology and Medicine,* 43**,** 645-657.

BURKE, S. P., SMITH, L. & SMITH, J. B. 2010. cIAP1 cooperatively inhibits procaspase-3 activation by the caspase-9 apoptosome. *Journal of Biological Chemistry***,** jbc. M110. 125955.

CHU, Y.-L., HO, C.-T., CHUNG, J.-G., RAJASEKARAN, R. & SHEEN, L.-Y. 2012. Allicin induces p53-mediated autophagy in Hep G2 human liver cancer cells. *Journal of agricultural and food chemistry,* 60**,** 8363-8371.

CHUTURGOON, A., PHULUKDAREE, A. & MOODLEY, D. 2014. Fumonisin B1 induces global DNA hypomethylation in HepG2 cells–An alternative mechanism of action. *Toxicology,* 315**,** 65-69.

CHUTURGOON, A. A., PHULUKDAREE, A. & MOODLEY, D. 2015. Fumonisin B1 inhibits apoptosis in HepG2 cells by inducing Birc-8/ILP-2. *Toxicology letters,* 235**,** 67-74.

DE BAERE, S., CROUBELS, S., NOVAK, B., BICHL, G. & ANTONISSEN, G. 2018. Development and Validation of a UPLC-MS/MS and UPLC-HR-MS Method for the Determination of Fumonisin B1 and Its Hydrolysed Metabolites and Fumonisin B2 in Broiler Chicken Plasma. *Toxins,* 10**,** 62.

DEMIREL, G., ALPERTUNGA, B. & OZDEN, S. 2015. Role of fumonisin B1 on DNA methylation changes in rat kidney and liver cells. *Pharmaceutical biology,* 53**,** 1302-1310.

DOMIJAN, A.-M. 2012. Fumonisin B1: a neurotoxic mycotoxin/fumonizin B1: Neurotoksični Mikotoksin. *Archives of Industrial Hygiene and Toxicology,* 63**,** 531-544.

DRAGAN, Y. P., BIDLACK, W. R., COHEN, S. M., GOLDSWORTHY, T. L., HARD, G. C., HOWARD, P. C., RILEY, R. T. & VOSS, K. A. 2001. Implications of apoptosis for toxicity, carcinogenicity, and risk assessment: fumonisin B1 as an example. *Toxicological Sciences,* 61**,** 6-17.

EL GOLLI-BENNOUR, E. & BACHA, H. 2011. Hsp70 expression as biomarkers of oxidative stress: Mycotoxins' exploration. *Toxicology,* 287**,** 1-7.

ELMORE, S. 2007. Apoptosis: a review of programmed cell death. *Toxicologic pathology,* 35**,** 495-516.

FINK-GRERNMELS, J. 1999. Mycotoxins: their implications for human and animal health. *Veterinary Quarterly,* 21**,** 115-120.

FORMAN, H. J., ZHANG, H. & RINNA, A. 2009. Glutathione: overview of its protective roles, measurement, and biosynthesis. *Molecular aspects of medicine,* 30**,** 1-12.

FUKAI, T. & USHIO-FUKAI, M. 2011. Superoxide dismutases: role in redox signaling, vascular function, and diseases. *Antioxidants & redox signaling,* 15**,** 1583-1606.

GARCÍA-TREJO, E., ARELLANO-BUENDÍA, A. S., ARGÜELLO-GARCÍA, R., LOREDO-MENDOZA, M. L., GARCÍA-ARROYO, F. E., ARELLANO-MENDOZA, M. G., CASTILLO-HERNÁNDEZ, M. C., GUEVARA-BALCÁZAR, G., TAPIA, E. & SÁNCHEZ-LOZADA, L. G. 2016. Effects of allicin on hypertension and cardiac function in chronic kidney disease. *Oxidative medicine and cellular longevity,* 2016.

GARRIDO, C. & KROEMER, G. 2004. Life's smile, death's grin: vital functions of apoptosis-executing proteins. *Current opinion in cell biology,* 16**,** 639-646.

GELDERBLOM, W., ABEL, S., SMUTS, C. M., MARNEWICK, J., MARASAS, W., LEMMER, E. R. & RAMLJAK, D. 2001. Fumonisin-induced hepatocarcinogenesis: mechanisms related to cancer initiation and promotion. *Environmental health perspectives,* 109**,** 291.

GELDERBLOM, W., JASKIEWICZ, K., MARASAS, W., THIEL, P., HORAK, R., VLEGGAAR, R. & KRIEK, N. 1988. Fumonisins--novel mycotoxins with cancer-promoting activity produced by Fusarium moniliforme. *Applied and environmental microbiology,* 54**,** 1806-1811.

GODARD, T., DESLANDES, E., LEBAILLY, P., VIGREUX, C., POULAIN, L., SICHEL, F., POUL, J. M. & GAUDUCHON, P. 1999. Comet assay and DNA flow cytometry analysis of staurosporine-induced apoptosis. *Cytometry: The Journal of the International Society for Analytical Cytology,* 36**,** 117-122.

GOVENDER, M. 2016. *Fusaric acid dampens the Nrf2-mediated stress response in human embryonic kidney cells.*

GREENWELL, M. & RAHMAN, P. 2015. Medicinal plants: their use in anticancer treatment. *International journal of pharmaceutical sciences and research,* 6**,** 4103.

GRUHLKE, M. C., NICCO, C., BATTEUX, F. & SLUSARENKO, A. J. 2016. The effects of allicin, a reactive sulfur species from garlic, on a selection of mammalian cell lines. *Antioxidants,* 6**,** 1.

GUMPRECHT, L. A., MARCUCCI, A., WEIGEL, R. M., VESONDER, R. F., RILEY, R. T., SHOWKER, J. L., BEASLEY, V. R. & HASCHEK, W. M. 1995. Effects of intravenous fumonisin B1 in rabbits: Nephrotoxicityxs and sphingolipid alterations. *Natural toxins,* 3**,** 395-403.

GUPTA, R. K., PATEL, A. K., SHAH, N., CHAUDHARY, A., JHA, U., YADAV, U. C., GUPTA, P. K. & PAKUWAL, U. 2014. Oxidative stress and antioxidants in disease and cancer. *Asian Pac Cancer Prev,* 15**,** 4405-4409.

HA, M. & YUAN, Y. 2004. Allicin induced cell cycle arrest in human gastric cancer cell lines. *Zhonghua zhong liu za zhi [Chinese journal of oncology],* 26**,** 585-589.

HALLIWELL, B. 2007. Biochemistry of oxidative stress. Portland Press Limited.

HALUŠKOVÁ, J. 2010. Epigenetic studies in human diseases. *Folia biologica (Praha),* 56**,** 83-96.

HARRISON, L. R., COLVIN, B. M., GREENE, J. T., NEWMAN, L. E. & COLE JR, J. R. 1990. Pulmonary edema and hydrothorax in swine produced by fumonisin B1, a toxic metabolite of Fusarium moniliforme. *Journal of Veterinary Diagnostic Investigation,* 2**,** 217-221.

HASSAN, A. M., ABDEL-AZIEM, S. H., EL-NEKEETY, A. A. & ABDEL-WAHHAB, M. A. 2015. Panaxginseng extract modulates oxidative stress, DNA fragmentation and up-regulate gene expression in rats sub chronically treated with aflatoxin B1 and fumonisin B1. *Cytotechnology,* 67**,** 861-871.

HASSAN, M., WATARI, H., ABUALMAATY, A., OHBA, Y. & SAKURAGI, N. 2014. Apoptosis and molecular targeting therapy in cancer. *BioMed research international,* 2014.

HASTINGS, J. 1968. Bioluminescence. *Annual review of biochemistry,* 37**,** 597-630.

HELD, P. 2012. An introduction to reactive oxygen species. *Tech Resources-App Guides,* 802**,** 5-9.

HENDRICKS, K. 1999. Fumonisins and neural tube defects in south Texas. *Epidemiology***,** 198-200.

HERNANDEZ-RODRIGUEZ, P. & RAMIREZ, A. G. 2012. Polymerase chain reaction: types, utilities and limitations. *Polymerase Chain Reaction.* InTech.

HIRSCH, K., DANILENKO, M., GIAT, J., MIRON, T., RABINKOV, A., WILCHEK, M., MIRELMAN, D., LEVY, J. & SHARONI, Y. 2000. Effect of purified allicin, the major ingredient offreshly crushed garlic, on cancer cell proliferation. *Nutrition and cancer,* 38**,** 245-254.

HOWARD, P. C., EPPLEY, R. M., STACK, M. E., WARBRITTON, A., VOSS, K. A., LORENTZEN, R. J., KOVACH, R. M. & BUCCI, T. J. 2001. Fumonisin b1 carcinogenicity in a two-year feeding study using F344 rats and B6C3F1 mice. *Environmental Health Perspectives,* 109**,** 277.

HUMPF, H. U. & VOSS, K. A. 2004. Effects of thermal food processing on the chemical structure and toxicity of fumonisin mycotoxins. *Molecular nutrition & food research,* 48**,** 255-269.

ICIEK, M., KWIECIEŃ, I. & WŁODEK, L. 2009. Biological properties of garlic and garlic-derived organosulfur compounds. *Environmental and molecular mutagenesis,* 50**,** 247-265.

KELLERMAN, T. S., MARASAS, W., THIEL, P., GELDERBLOM, W., CAWOOD, M. & COETZER, J. 1990. Leukoencephalomalacia in two horses induced by oral dosing of fumonisin B1. *The Onderstepoort journal of veterinary research,* 57**,** 269-275.

KERR, J. F., WYLLIE, A. H. & CURRIE, A. R. 1972. Apoptosis: a basic biological phenomenon with wideranging implications in tissue kinetics. *British journal of cancer,* 26**,** 239.

KHAN, R., PHULUKDAREE, A. & CHUTURGOON, A. 2018a. Concentration-dependent effect of fumonisin B1 on apoptosis in oesophageal cancer cells. *Human & experimental toxicology,* 37**,** 762-771.

KHAN, R. B., PHULUKDAREE, A. & CHUTURGOON, A. A. 2018b. Fumonisin B1 induces oxidative stress in oesophageal (SNO) cancer cells. *Toxicon,* 141**,** 104-111.

KLARIĆ, M. Š., PEPELJNJAK, S., DOMIJAN, A. M. & PETRIK, J. 2007. Lipid peroxidation and glutathione levels in porcine kidney PK15 cells after individual and combined treatment with fumonisin B1, beauvericin and ochratoxin A. *Basic & clinical pharmacology & toxicology,* 100**,** 157-164.

KÓCSÓ, D. J., SZABÓ-FODOR, J., MÉZES, M., BALOGH, K., FERENCZI, S., SZABÓ, A., BÓTA, B. & KOVÁCS, M. 2018. Fumonisin B1 exposure increases Hsp70 expression in the lung and kidney of rats without inducing significant oxidative stress. *Acta Veterinaria Hungarica,* 66**,** 394-407.

KOFF, J. L., RAMACHANDIRAN, S. & BERNAL-MIZRACHI, L. 2015. A time to kill: targeting apoptosis in cancer. *International journal of molecular sciences,* 16**,** 2942-2955.

KRUEGER, K., SHEN, J., MAIER, A., TEPEL, M. & SCHOLZE, A. 2016. Lower superoxide dismutase 2 (SOD2) protein content in mononuclear cells is associated with better survival in patients with hemodialysis therapy. *Oxidative Medicine and Cellular Longevity,* 2016.

LASH, L. H. 2005. Role of glutathione transport processes in kidney function. *Toxicology and applied pharmacology,* 204**,** 329-342.

LIAO, Y., CHEN, J., TANG, W., GE, Q., LU, Q. & YANG, Z. 2009. Effect of P38MAPK signal transduction pathway on apoptosis of THP-1 induced by allicin. *Zhongguo Zhong yao za zhi= Zhongguo zhongyao zazhi= China journal of Chinese materia medica,* 34**,** 1439-1443.

LIVAK, K. J. & SCHMITTGEN, T. D. 2001. Analysis of relative gene expression data using real-time quantitative PCR and the 2− ΔΔCT method. *methods,* 25**,** 402-408.

LUNDIN, A. 2000. Use of firefly luciferase in ATP-related assays of biomass, enzymes, and metabolites.

LUO, R., FANG, D., HANG, H. & TANG, Z. 2016. The mechanism in gastric cancer chemoprevention by allicin. *Anti-Cancer Agents in Medicinal Chemistry (Formerly Current Medicinal Chemistry-Anti-Cancer Agents),* 16**,** 802-809.

LUSHCHAK, V. 2015. Free radicals, reactive oxygen species, oxidative stresses and their classifications. *The Ukrainian Biochemical Journal***,** 11-18.

MA, Q. 2013. Role of nrf2 in oxidative stress and toxicity. *Annual review of pharmacology and toxicology,* 53**,** 401-426.

MAHMOOD, T. & YANG, P.-C. 2012. Western blot: technique, theory, and trouble shooting. *North American journal of medical sciences,* 4**,** 429.

MARASAS, D. & WFO, J. 1988. Fusarium moniliforme contamination of maize in oesophageal cancer areas in Transkei. *South African Medical Journal,* 74**,** 110-114.

MARASAS, W. F., RILEY, R. T., HENDRICKS, K. A., STEVENS, V. L., SADLER, T. W., GELINEAU-VAN WAES, J., MISSMER, S. A., CABRERA, J., TORRES, O. & GELDERBLOM, W. C. 2004. Fumonisins disrupt sphingolipid metabolism, folate transport, and neural tube development in embryo culture and in vivo: a potential risk factor for human neural tube defects among populations consuming fumonisin-contaminated maize. *The Journal of nutrition,* 134**,** 711-716.

MARASAS, W. F. O., KELLERMAN, T. S., GELDERBLOM, W. C., THIEL, P., VAN DER LUGT, J. J. & COETZER, J. A. 1988. Leukoencephalomalacia in a horse induced by fumonisin B_1 isolated from Fusarium moniliforme.

MARASAS, W. F. O., KELLERMAN, T. S., GELDERBLOM, W. C., THIEL, P., VAN DER LUGT, J. J. & COETZER, J. A. 2014. Leukoencephalomalacia in a horse induced by fumonisin B_1 isolated from Fusarium moniliforme.

MATUR, E., ERGUL, E., AKYAZI, I., ERASLAN, E., INAL, G., BILGIC, S. & DEMIRCAN, H. 2011. Effects of Saccharomyces cerevisiae extract on haematological parameters, immune function and the antioxidant defence system in breeder hens fed aflatoxin contaminated diets. *British poultry science,* 52**,** 541-550.

MEHTA, R. L., KELLUM, J. A., SHAH, S. V., MOLITORIS, B. A., RONCO, C., WARNOCK, D. G. & LEVIN, A. 2007. Acute Kidney Injury Network: report of an initiative to improve outcomes in acute kidney injury. *Critical care,* 11**,** R31.

MERKSAMER, P. I., LIU, Y., HE, W., HIRSCHEY, M. D., CHEN, D. & VERDIN, E. 2013. The sirtuins, oxidative stress and aging: an emerging link. *Aging (Albany NY),* 5**,** 144.

MERRILL, A. H. 2002. De novo sphingolipid biosynthesis: a necessary, but dangerous, pathway. *Journal of Biological Chemistry,* 277**,** 25843-25846.

MERRILL JR, A. H., SULLARDS, M. C., WANG, E., VOSS, K. A. & RILEY, R. T. 2001. Sphingolipid metabolism: roles in signal transduction and disruption by fumonisins. *Environmental health perspectives,* 109**,** 283.

MIKAILI, P., MAADIRAD, S., MOLOUDIZARGARI, M., AGHAJANSHAKERI, S. & SARAHROODI, S. 2013. Therapeutic uses and pharmacological properties of garlic, shallot, and their biologically active compounds. *Iranian journal of basic medical sciences,* 16**,** 1031.

MILLER, J. D., SAVARD, M. E., SIBILIA, A., RAPIOR, S., HOCKING, A. D. & PITT, J. I. 1993. Production of fumonisins and fusarins by Fusarium moniliforme from Southeast Asia. *Mycologia***,** 385-391.

MINERVINI, F., FORNELLI, F. & FLYNN, K. 2004. Toxicity and apoptosis induced by the mycotoxins nivalenol, deoxynivalenol and fumonisin B1 in a human erythroleukemia cell line. *Toxicology in Vitro,* 18**,** 21-28.

MISSMER, S. A., SUAREZ, L., FELKNER, M., WANG, E., MERRILL JR, A. H., ROTHMAN, K. J. & HENDRICKS, K. A. 2005. Exposure to fumonisins and the occurrence of neural tube defects along the Texas–Mexico border. *Environmental health perspectives,* 114**,** 237-241.

MUKHOPADHYAY, S., PANDA, P. K., SINHA, N., DAS, D. N. & BHUTIA, S. K. 2014. Autophagy and apoptosis: where do they meet? *Apoptosis,* 19**,** 555-566.

MYBURG, R. B., DUTTON, M. F. & CHUTURGOON, A. A. 2002. Cytotoxicity of fumonisin B1, diethylnitrosamine, and catechol on the SNO esophageal cancer cell line. *Environmental health perspectives,* 110**,** 813-815.

MYTILINEOU, C., KRAMER, B. C. & YABUT, J. A. 2002. Glutathione depletion and oxidative stress. *Parkinsonism & related disorders,* 8**,** 385-387.

OAKES, K. D. & VAN DER KRAAK, G. J. 2003. Utility of the TBARS assay in detecting oxidative stress in white sucker (Catostomus commersoni) populations exposed to pulp mill effluent. *Aquatic Toxicology,* 63**,** 447-463.

OOMMEN, S., ANTO, R. J., SRINIVAS, G. & KARUNAGARAN, D. 2004. Allicin (from garlic) induces caspase-mediated apoptosis in cancer cells. *European journal of pharmacology,* 485**,** 97-103.

PARK, S.-Y., CHO, S.-J., KWON, H.-C., LEE, K.-R., RHEE, D.-K. & PYO, S. 2005. Caspase-independent cell death by allicin in human epithelial carcinoma cells: involvement of PKA. *Cancer Letters,* 224**,** 123-132.

PARRISH, A. B., FREEL, C. D. & KORNBLUTH, S. 2013. Cellular mechanisms controlling caspase activation and function. *Cold Spring Harbor perspectives in biology,* 5**,** a008672.

PATRA, K. C. & HAY, N. 2014. The pentose phosphate pathway and cancer. *Trends in biochemical sciences,* 39**,** 347-354.

PRAGER-KHOUTORSKY, M., GONCHAROV, I., RABINKOV, A., MIRELMAN, D., GEIGER, B. & BERSHADSKY, A. D. 2007. Allicin inhibits cell polarization, migration and division via its direct effect on microtubules. *Cell motility and the cytoskeleton,* 64**,** 321-337.

RENEHAN, A. G., BOOTH, C. & POTTEN, C. S. 2001. What is apoptosis, and why is it important? *BMJ: British Medical Journal,* 322**,** 1536.

RHEEDER, J., MARASAS, W., THIEL, P., SYDENHAM, E., SHEPHARD, G. & VAN SCHALKWYK, D. 1992. Fusarium moniliforme and fumonisins in corn in relation to human esophageal cancer in Transkei.

RILEY, R. T., HINTON, D. M., CHAMBERLAIN, W. J., BACON, C. W., WANG, E., MERRILL JR, A. H. & VOSS, K. A. 1994. Dietary fumonisin B1 induces disruption of sphingolipid metabolism in Sprague-Dawley rats: a new mechanism of nephrotoxicity. *The Journal of nutrition,* 124**,** 594-603.

RISS, T., MORAVEC, R., NILES, A., BENINK, H., WORZELLA, T. & MINOR, L. 2004. Cell Viability Assays, 2015. *Google Scholar*.

RONKEN, S. S. 2009. Influence of material choice and surface structure on cell behaviour.

RUMORA, L., KOVAČIĆ, S., ROZGAJ, R., ČEPELAK, I., PEPELJNJAK, S. & GRUBIŠIĆ, T. Ž. 2002. Cytotoxic and genotoxic effects of fumonisin B 1 on rabbit kidney RK13 cell line. *Archives of toxicology,* 76**,** 55-61.

SANCAK, D. & OZDEN, S. 2015. Global histone modifications in fumonisin B1 exposure in rat kidney epithelial cells. *Toxicology in Vitro,* 29**,** 1809-1815.

SCHMALE, D. G. & MUNKVOLD, G. P. 2009. Mycotoxins in crops: A threat to human and domestic animal health. *The plant health instructor,* 3**,** 340-353.

SCHOLZE, A., KRUEGER, K., DIEDRICH, M., RÄTH, C., TORGES, A., JANKOWSKI, V., MAIER, A., THILO, F., ZIDEK, W. & TEPEL, M. 2011. Superoxide dismutase type 1 in monocytes of chronic kidney disease patients. *Amino Acids,* 41**,** 427-438.

SEEFELDER, W., HUMPF, H.-U., SCHWERDT, G., FREUDINGER, R. & GEKLE, M. 2003. Induction of apoptosis in cultured human proximal tubule cells by fumonisins and fumonisin metabolites. *Toxicology and applied pharmacology,* 192**,** 146-153.

SHARMA, S., KELLY, T. K. & JONES, P. A. 2010. Epigenetics in cancer. *Carcinogenesis,* 31**,** 27-36.

SHI, Y. 2004. Caspase activation: revisiting the induced proximity model. *Cell,* 117**,** 855-858.

SHUNMUGAM, L. 2016. *Moringa oleifera crude aqueous leaf extract induces apoptosis in human hepatocellular carcinoma cells via the upregulation of NF-kB and IL-6/STAT3 pathway.*

SIEGERS, C.-P., STEFFEN, B., RÖBKE, A. & PENTZ, R. 1999. The effects of garlic preparations against human tumor cell proliferation. *Phytomedicine,* 6**,** 7-11.

SINGH, N. P., MCCOY, M. T., TICE, R. R. & SCHNEIDER, E. L. 1988. A simple technique for quantitation of low levels of DNA damage in individual cells. *Experimental cell research,* 175**,** 184-191.

STOCKMANN-JUVALA, H. & SAVOLAINEN, K. 2008. A review of the toxic effects and mechanisms of action of fumonisin B1. *Human & experimental toxicology,* 27**,** 799-809.

SUDDEK, G. M. 2014. Allicin enhances chemotherapeutic response and ameliorates tamoxifen-induced liver injury in experimental animals. *Pharmaceutical biology,* 52**,** 1009-1014.

SUN, G., WANG, S., HU, X., SU, J., HUANG, T., YU, J., TANG, L., GAO, W. & WANG, J.-S. 2007. Fumonisin B1 contamination of home-grown corn in high-risk areas for esophageal and liver cancer in China. *Food additives and contaminants,* 24**,** 181-185.

SYDENHAM, E. W., THIEL, P. G., MARASAS, W. F., SHEPHARD, G. S., VAN SCHALKWYK, D. J. & KOCH, K. R. 1990. Natural occurrence of some Fusarium mycotoxins in corn from low and high esophageal cancer prevalence areas of the Transkei, Southern Africa. *Journal of Agricultural and Food Chemistry,* 38**,** 1900-1903.

TOWNER, R. A., QIAN, S. Y., KADIISKA, M. B. & MASON, R. P. 2003. In vivo identification of aflatoxin-induced free radicals in rat bile. *Free Radical Biology and Medicine,* 35**,** 1330-1340.

TRYPHONAS, H., BONDY, G., MILLER, J., LACROIX, F., HODGEN, M., MCGUIRE, P., FERNIE, S., MILLER, D. & HAYWARD, S. 1997. Effects of fumonisin B1 on the immune system of Sprague-Dawley rats following a 14-day oral (gavage) exposure. *Toxicological Sciences,* 39**,** 53-59.

VAN DER WESTHUIZEN, L., SHEPHARD, G., RHEEDER, J. & BURGER, H.-M. 2010. Individual fumonisin exposure and sphingoid base levels in rural populations consuming maize in South Africa. *Food and Chemical Toxicology,* 48**,** 1698-1703.

VOSS, K. A., CHAMBERLAIN, W. J., BACON, C. W. & NORRED, W. P. 1993. A preliminary investigation on renal and hepatic toxicity in rats fed purified fumonisin B1. *Natural toxins,* 1**,** 222-228.

VOSS, K. A., CHAMBERLAIN, W. J., BACON, C. W., RILEY, R. T. & NORRED, W. P. 1995. Subchronic toxicity of fumonisin B1 to male and female rats. *Food Additives & Contaminants,* 12**,** 473-478.

VOSS, K. A. & RILEY, R. T. 2013. Fumonisin toxicity and mechanism of action: overview and current perspectives. *Food Safety,* 1**,** 2013006-2013006.

WANG, E., NORRED, W., BACON, C., RILEY, R. & MERRILL, A. H. 1991. Inhibition of sphingolipid biosynthesis by fumonisins. Implications for diseases associated with Fusarium moniliforme. *Journal of Biological Chemistry,* 266**,** 14486-14490.

YOSHIZAWA, T., YAMASHITA, A. & LUO, Y. 1994. Fumonisin occurrence in corn from high- and low-risk areas for human esophageal cancer in China. *Applied and Environmental Microbiology,* 60**,** 1626-1629.

ZITKA, O., SKALICKOVA, S., GUMULEC, J., MASARIK, M., ADAM, V., HUBALEK, J., TRNKOVA, L., KRUSEOVA, J., ECKSCHLAGER, T. & KIZEK, R. 2012. Redox status expressed as GSH: GSSG ratio as a marker for oxidative stress in paediatric tumour patients. *Oncology letters,* 4**,** 1247-1253.

APPENDICES

Appendix A: Nitric oxide assay

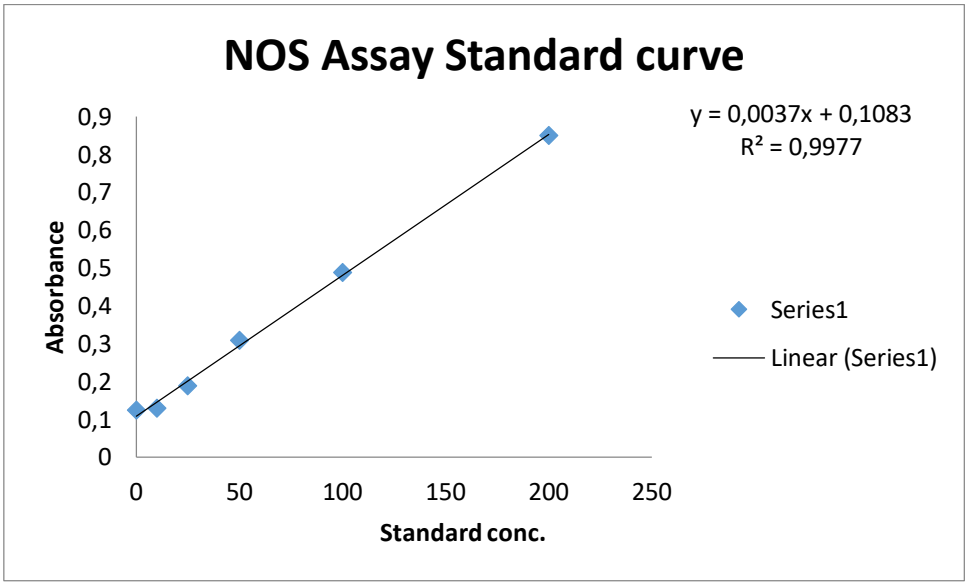

Figure 1: Mean absorbance values of NOS standard curve

Appendix B: Glutathione (GSH) Assay

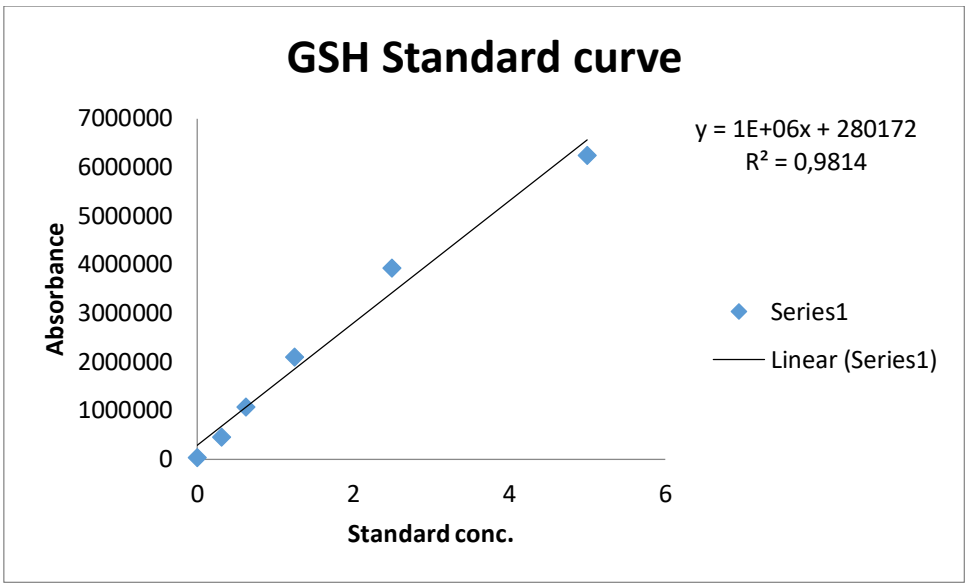

Figure 1: Mean absorbance values of GSH concentrations standard curve.

Appendix C: Protein standardisation

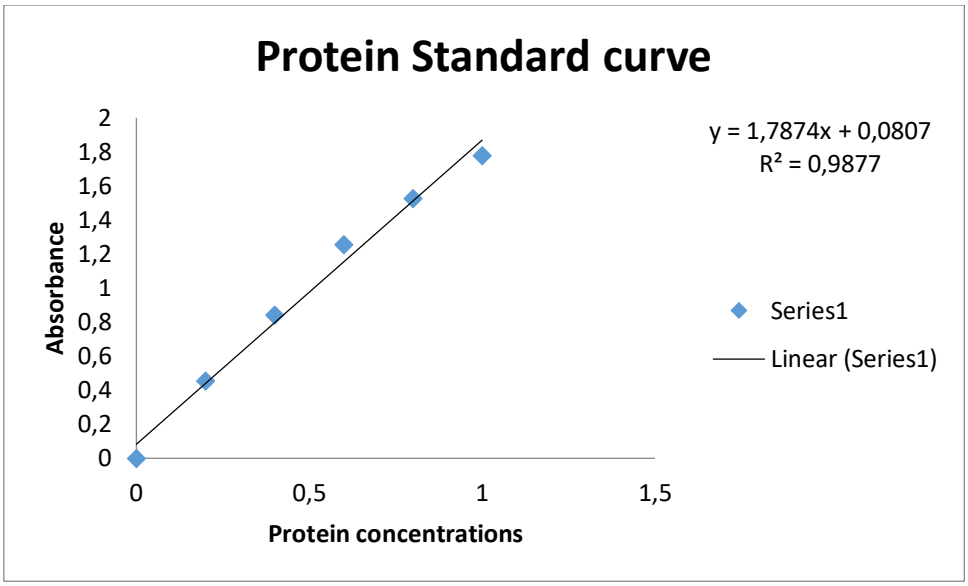

Figure 1: Standard curve for protein standardisation